Necroptosis promotes the Aging of the Male Reproductive System in Mice

Dianrong Li, Lingjun Meng, Tao Xu, Yaning Su, Xiao Liu, Zhiyuan Zhang, Xiaodong Wang*

National Institute of Biological Sciences, 7 Science Park Road, Zhongguancun Life Science Park, Beijing 102206, China

*For correspondence: wangxiaodong@nibs.ac.cn

Abstract

Necroptosis is a form of programmed necrotic cell death in mammals that is mediated by a pair of kinases, RIP1 and RIP3, as well as the RIP3 substrate MLKL. We report here that male reproductive organs of both RIP3- and MLKL-knockout mice retain "youthful" morphology and function into advanced age, while those of age-matched wild type mice deteriorate. The RIP3 phosphorylation of MLKL, the activation marker of necroptosis, is detected in spermatogonial stem cells in the testes of old but not in young wild type mice. When the testes of young wild type mice are given a local necroptotic stimulus, their reproductive organs showed accelerated aging. Feeding of wild type mice with an RIP1 inhibitor prior to the normal onset of age-related changes in their reproductive organs blocked the appearance of signs of aging. Thus, necroptosis in testes promotes the aging-associated deterioration of the male reproductive system in mice.

Introduction

Necroptosis is a form of programmed necrotic cell death caused by the tumor necrosis factor family of cytokines (Christofferson and Yuan, 2010; Vandenabeele et al., 2010). In response to the activation of TNF receptor family members, receptor-interacting kinase 1 (RIP1) is recruited to the cytosolic side of the receptor and its kinase activity is activated (Holler et al., 2000). RIP1 then interacts with and phosphorylates a related kinase, RIP3, leading to its activation (Cho et al., 2009; Degterev et al., 2008; He et al., 2009; Zhang et al., 2009). If the cells also happen to have their caspase-8 activity inhibited, either through interaction with its cellular inhibitor cFLIP or through the action of viral or chemical inhibitors, RIP3 drives the cell fate towards necroptosis (He et al., 2009; Holler et al., 2000). Necroptosis can be inhibited by RIP1 kinase inhibitor compounds, and can be promoted by small molecule Smac mimetics, which shifts RIP1 function from NF-κB activation to activation of RIP3 (Degterev et al., 2008; Wang et al., 2008). Once active, RIP3 then phosphorylates a pseudokinase called mixed lineage kinase domain-like protein (MLKL) (Sun et al., 2012). MLKL normally exists as an inactive monomer in the cytosol. Upon RIP3 phosphorylation on serine 357 and threonine 358 of human MLKL or the mouse equivalent of serine 345, serine 347, and threonine 349, MLKL forms oligomers and translocates to the plasma membrane, where it disrupts membrane integrity, resulting in necrotic cell death (Cai et al., 2014; Chen et al., 2014; Rodriguez et al., 2016; Sun et al., 2012; Wang et al., 2014).

Necroptosis is known to have important functions under pathological conditions of microbial infections or tissue damage since RIP3 knockout mice show defects in defending microbial infections or manifest less tissue damage in a variety of chemical or ischemic reperfusion induced tissue damage models (Cho et al., 2009; He et al., 2009; Robinson et al.,

2012; Upton et al., 2010; Zhou and Yuan, 2014). However, mice with RIP3 or MLKL gene knockout are remarkably normal without any noticeable developmental, physiological, or fertility defects (Murphy et al., 2013; Newton et al., 2004; Wu et al., 2013). Therefore, under what physiological conditions necroptosis happens in which tissue remains the biggest unanswered question in this research field.

While conducting a study investigating the impact of necroptosis on the progression of atherosclerosis (Meng et al., 2015), we serendipitously found that the male reproductive organ of mice with RIP3 and MLKL knockout looked remarkably young even at advanced ages. A comprehensive follow up study present here revealed that necroptosis functions in promoting the aging of male reproductive system in mice.

Results

The aging of reproductive organs is delayed in RIP3-knockout mice

We first noticed that the 18-month old RIP3-knockout ($RIP3^{-/-}$) mice of the C57BL/6 strain looked thinner than the age-matched wild type (WT, $RIP3^{+/+}$) mice of the same strain that were housed under the same conditions (Figure 1A). The average weight of 18-month old wild type mice was 46 grams, significantly more than of 37 grams of weight of the age-matched RIP3-knockout mice (Figure 1B). The weights of 4-month old wild type and RIP3-knockout mice, on the other hand, were indistinguishable (Figure 1B). In addition to differences in whole body weights, the seminal vesicles, an auxiliary gland in the mouse male reproductive system, appeared to be quite different between 18-month old RIP3-knockout and wild type mice (Figure 1C). The weights of the seminal vesicles from 18-month old wild type mice (n=33) ranged from

~1,000 mg to 4,500 mg, while the weights of the same organ from the age-matched RIP3-knockout mice (n=30) were mostly below 1,000 mg (Figure 1D).

It is known that seminal vesicles become enlarged as mice get old (Finch and Girgis, 1974; Pettan-Brewer and Treuting, 2011). The difference in seminal vesicles from wild type and RIP3-knockout mice become noticeable after one year of life, and become increasingly evident over time. The seminal vesicles from wild type mice continue to grow, whereas the seminal vesicles from the RIP3-knockout mice did not change in size from 4 months to 24 months (Figure 1-figure supplement 1A, 1B). There were no obvious differences in the overall anatomical structure of seminal vesicles between wild type and RIP3-knockout mice (Figure 1C and Figure 1-figure supplement 1A). Close examination revealed that the epithelium of the seminal vesicles from 18-month old wild type mice showed irregularities, with spaces separating the epithelium and the liquid compartment, whereas the seminal-vesicle epithelial cells from the age-matched RIP3-knockout mice were tightly packed, just as they are in young mice (Figure 1-figure supplement 1C)

The seminal vesicles of mice are anatomically simple, consisting of only an epithelial layer that envelopes a liquid compartment (Gonzales, 2001). Therefore, the difference in seminal vesicles between wild type and RIP3-knockout mice did not offer much mechanistic insight what caused such a phenotype. We further studied the testes of wild type and RIP3-knockout mice. By the time mice reached 18 months of age, the wild type testes started to appear atrophic, and weighed less than RIP3-knockout testes (Figure 1-figure supplement 1D, 1E). Consistently, the testosterone level showed a dramatic drop as wild type mice aged from 4 to 18 months, whereas the testosterone levels hardly decreased at all in RIP3-knockout mice over the same period (Figure 1E). Moreover, the typical age-related increase in sex hormone-binding globulin (SHBG)

(Vermeulen et al., 1996) that is known to occur in wild type mice was not observed in RIP3-knockout mice (Figure 1-figure supplement 2A). Interestingly, the levels of two endocrine factors secreted by the pituitary gland, LH and FSH (Cooke and Saunders, 2002), did not differ between wild type and RIP3-knockout mice; both dropped significantly as mice aged from 4 months to 18 months (Figure 1-figure supplement 2B, 2C). This finding indicated that the difference in aging of reproductive system between old wild type and RIP3-knockout mice may result from local changes in testis.

Unlike what often happens in human upon reproductive organ aging, we did not notice any apparent anatomical difference in the anterior, dorsal, ventral, or lateral prostate by an hematoxylin and eosin (H&E) staining of mouse prostates (Pettan-Brewer and Treuting, 2011) sections of young (4-month) or old (18-month) mice of either the wild type or RIP3-knockout genotypes (Figure 1-figure supplement 3).

Knockout of RIP3 prevents the depletion of cells in the seminiferous tubules in aged testes

As a male mouse becomes sexually mature, the central lumens of seminiferous tubules in its testes begin to fill with sperm generated from the surrounding spermatogonial stem cells. The spermatogonial stem cells and spermatocytes are supported by Sertoli cells, which provide trophic factors and structural support for spermatogenesis (Cooke and Saunders, 2002). Sperm are then transferred and stored in the epididymis, from where mature sperm are ejected. After mixing with fluids from the seminal vesicles and prostate, the sperm travel alone the ejaculation track, where semen is formed (Cooke and Saunders, 2002).

When testes from 4-month old and 18-month old wild type and RIP3-knockout mice were dissected and their cross sections were examined under a microscope, cells in many of the

seminiferous tubules from the 18-month old wild type mice were lost, given the seminiferous tubules an "empty" appearance (Figure 1F, 1G). In contrast, the central lumens of the seminiferous tubules of 4-month old wild type and RIP3-knockout mice are fully surrounded with cells, and are filled with sperm. Strikingly, the seminiferous tubules of 18-month old RIP3-knockout mice looked no different than those of 4-month old mice (Figure 1F, 1G). Even more dramatically, when testis sections from 36-month old mice were examined, close to half of seminiferous tubules of wild type mice were empty, while more than 90% of those from the RIP3-knockout mice still appeared normal (Figure 1-figure supplement 4).

Sperm from the seminiferous tubules travel to the epididymis, where they mature and are stored prior to ejaculation (Cooke and Saunders, 2002). Similar to the phenotypes observed in the seminiferous tubules, most of the epididymides from 18-month old wild type mice had few sperm, whereas most of the epididymides of age-matched RIP3-knockout mice were full of sperm (Figure 1-figure supplement 5A). The sperm counts in epididymes increased steadily during development and peaked at four months of age, and there was little difference in the sperm counts between wild type and RIP3-knockout mice up to this time (Figure 1-figure supplement 5B). The sperm counts of wild type mice then started to decline, while those of RIP3-knockout mice remained steady until 12 months of age. Even at 24 months, the sperm counts of RIP3-knockout mice were still comparable with those of 4-month old wild type mice (Figure 1-figure supplement 5B).

Knockout of RIP3 prevents age-associated decline of reproductive capacity

To test if the sperm from aged RIP3-knockout mice remain functional, we set up breeding experiments that mated 4-month old, 13-month old, and 18-month old male mice with

pairs of 10-week old wild type female mice. As summarized in Figure 1H, both wild type and RIP3-knockout 4-month old male mice were fully fertile, and both groups sired a similar number of pups (Figure 1-table supplement 1). However, for 13-month-old mice, only 9 of the 20 wild type male mice sired pups, while 18 out of 23 RIP3-knockout males remained fertile (Figure 1H and Figure 1-table supplement 1,2). The difference was even more obvious with the 18-month old male mice. Only 4 out of 22 wild type male mice were still fertile at this age, whereas 15 out of 22 RIP3-knockout male mice remained fertile (Figure 1H and Figure 1-table supplement 1). We subsequently measured the reproductive longevity of wild type and RIP3-knockout male mice by pairing a pair of 10-weeks old female mice with each male in a cage and switch out a fresh pair of females every other month (Hofmann et al., 2015). Monitoring of the age at which each male sired its last litter showed that wild type mice on average lost the ability to sire offspring around 16 months, while the RIP3-knockout mice did not lose this ability until 22 months (Figure 1I).

RIP3 expression in spermatogonia, spermatocytes and Sertoli cells in testis

To investigate the underlining mechanism responsible for the delayed reproductive system aging phenotype, we first examined RIP3 expression using immunohistochemistry methods (IHC). We noted that the cells inside wild type seminiferous tubules were stained positively with anti-RIP3 antibody (Figure 2-figure supplement 1). In contrast, no staining was seen in the seminiferous tubules of RIP3-knockout mice, confirming the specificity of the antibody (Figure 2-figure supplement 1).

The specific cell types from testes were further analyzed by co-immunostaining of testis sections from sexually-mature wild type mice (8-weeks) with antibodies against RIP3 and other

previously-described cell-type specific markers. RIP3 expression was apparent in germ line spermatogonia expressing UTF1 (Jung et al., 2014; van Bragt et al., 2008) and in Sertoli cells expressing GATA-1 (Tsai et al., 2006). The testosterone-producing Leydig cells (marked by the HSD3B1 as described in Chang et al., 2011) located outside of seminiferous tubules, however, did not express RIP3 (Figure 2A). The RIP3 expression in each of these cell types was further confirmed when testes were dissected and the cells were spread on a slide and analyzed again with co-immunostaining. The cell shapes changed due to spreading with this method, but the individual cells were more clearly visible. Consistent with the IHC staining results, spermatogonia and Sertoli cells were positive for RIP3 staining while Leydig cells were not (Figure 2B). Moreover, the primary spermatocytes within seminiferous tubules that were not marked by IHC were now clearly visible when stained with the specific marker SMAD3 (Hentrich et al., 2011), and these cells expressed RIP3 (Figure 2B). The fact that the cells within seminiferous tubules, the sperm-producing unit of testis, are all positive for RIP3 expression raised a possibility that the age-associated depletion of these cells is through necroptosis.

The RIP3 substrate MLKL is phosphorylated in the seminiferous tubules of aged wild type mice

Recall that RIP3 transduces the necroptosis signal by phosphorylating the serine 345 of pesudokinase MLKL, we used an antibody against phospho-serine 345 of MLKL to analyze the testes of young and old mice. Phosphorylated MLKL (phospho-MLKL) was detected in seminiferous tubules in cells surrounding the center lumens in testes of 18-month old wild type mice, whereas no phospho-MLKL was detected in the same tissue area of 8-week old wild type mice, nor in 18-month old RIP3-knockout mice (Figure 2C). A quantitative analysis of the

phospho-MLKL staining of each age and genotype group is shown in Figure 2D. The data clearly showed that necroptosis-activation marker, i.e. serine-345 phosphorylation, was present abundantly in the seminiferous tubules of old wild type mice but not in young and RIP3-knockout mice, thus suggesting that necroptosis of these RIP3-expressing cells in seminiferous tubules might trigger the aging of male sex organs. Consistently, phospho-MLKL was detected by western blotting in extracts from testes of 18- and 24-month old wild type mice but not in extracts from age-matched RIP3 knockout mice (Figure 2E).

To further identify the exact cell type in the aged seminiferous tubules that show positive marker of necroptosis, we co-stained the testis sections with antibodies that specifically mark the different cell types in seminiferous tubules. As shown in Figure 2F, spermatogonia that specifically expressing UTF1 were co-stained with the anti-phospho-MLKL antibody. On the other hand, Sertoli cells did not show phosphor-MLKL staining even though they do express RIP3. Not surprisingly, Leydig cells that do not have RIP3 expression also did not stain with the phosphor-MLKL antibody.

Activation of apoptosis in Leydig cells during aging

The sex hormone-producing Leydig cells in testes do not express RIP3, yet in old mice testis, the hormone level drops and Leydig cells are also gone. We therefore checked the cleavage status of procaspase-3 (a known marker of apoptosis) and procaspase-8 in the aged testes of wild type and RIP3-knockout mice using IHC. Cleaved procaspase-3 and Cleaved procaspase-8 was detected in the wild type Leydig cells of 18, and 36-month old mice, while no such signal was observed in age-matched RIP3-knockout mice (Figure 3A-3D and Figure3-figure supplement 1A,1B). The cleaved-Caspase-3 was also detected by western blotting using

205 extracts from the aged wild type testes but not in RIP3-knockout testes (Figure 3-figure
206 supplement 1C). It is thus likely that Leydig cells undergo apoptosis, as a secondary response to
207 necroptosis in seminiferous tubules during aging process.
208
209 **Caspase-8 levels decrease during aging in empty seminiferous tubules**

210 We also used immunohistochemistry methods to examine the caspase-8 level in relative
211 to RIP3 in testes of wild type mice of advanced age. In aged wild type mice, caspase-8 levels
212 decreased in the seminiferous tubules showing the sign of cell depletion (Figure 3E, 3F), and
213 increased in the Leydig cells (Figure3-figure supplement 2). This reduction in caspase-8 may
214 explain how it is that necroptosis, but not apoptosis, occurs in the seminiferous tubules of aged
215 mice.
216
217 **Knockout of MLKL also delays the aging of mouse reproductive organs**

218 The delayed testis aging phenotype of RIP3 knockout mice and detection of necrptosis
219 activation marker in spermatogonia in aged wild type mice suggest that necroptosis might be the
220 underlying cause of testis aging. To further investigate possibility, we also characterized the
221 aging-associated phenotype of MLKL knockout mice. We first weighed 15-month old wild type,
222 RIP3-knockout, and MLKL-knockout ($MLKL^{-/-}$) mice. There was no significant difference
223 between the weights of MLKL- and RIP3-knockout mice, and mice of both of these knockout
224 genotypes weighed less than wild type mice at this age (Figure 4A). We also analyzed seminal
225 vesicles and seminiferous tubules in aged MLKL-knockout mice (15-month old). Compared to
226 the obvious aging that had occurred in wild type mice, the seminal vesicles of MLKL-knockout
227 mice maintained a youthful appearance, exhibiting the same phenotype as RIP3-knockout mice

(Figure 4B). Furthermore, while the majority of seminal vesicles from 15-month old wild type mice weighed more than 1,000 milligrams, almost all of the seminal vesicles from age-matched MLKL- and RIP3-knockout weighed less than 1,000 milligrams (Figure 4C). Consistently, the testosterone levels of both MLKL- and RIP3-knockout mice were also significant higher than those of age-matched wild type mice (Figure 4D). Further, very few (<2%) of the seminiferous tubules from MLKL-knockout mice were empty at 15 months of age, similar to the tubules of RIP3-knockout mice, while more than 12% of seminiferous tubules from the age-matched wild type mice were already empty (Figure 4E, 4F). Finally, the fertility rates of both 16-Month old MLKL- and RIP3-knockout mice were also significant higher than those of age-matched wild type mice (Figure 4G).

Induction of necroptosis in testis depleted cells in seminiferous tubules

To directly demonstrate that necroptosis in testes is sufficient to cause the aging of the male reproductive system, we injected a combination of TNF-α, Smac mimetic, and caspase inhibitor z-VAD-FMK (henceforth 'TSZ')(He et al., 2009), a known necroptosis stimulus to the testes of 2-month old mice. Injection of TSZ directly into the testis induced MLKL phosphorylation (Figure 5A, 5B). Phospho-MLKL was obviously present within the seminiferous tubules of TSZ-injected wild type testes, but not TSZ-treated RIP3-knockout or MLKL-knockout testes, confirming the activation of necroptosis in testes following TSZ injection (Figure 5C). Moreover, when the cells were isolated from a wild type testis and then treated with TSZ prior to staining with antibodies against phospho-MLKL and cell-type specific markers, cells in the seminiferous tubules, including spermatogonia, Sertoli cells, and spermatocytes, were stained positive for phospho-MLKL, whereas Leydig cells outside

seminiferous tubules were negative (Figure 5-figure supplement 1). The consequences of necroptosis induction in testes became apparent 72 hours after a single TSZ injection. By this point, about 25% of wild type seminiferous tubules were empty, whereas almost none of the seminiferous tubules from RIP3- and MLKL-knockout mice were affected (Figure 5D, 5E).

Induction of necroptosis in testes accelerates aging of the male reproductive system

In addition to monitoring these short-term effects following TSZ injection of 3-month-old mice, we waited for three additional months following the injection and assessed the long-term effects of induced necroptosis in mouse testes. Interestingly, three months after TSZ injection, the seminal vesicles of wild type recipient mice were as enlarged as those from mice older than 15 months. However, no such enlargement of seminal vesicles was observed in RIP3- and MLKL-knockout mice after the same TSZ treatment of their testes (Figure 6A, 6B). Additionally, more than 30% of the wild type seminiferous tubules remained empty three months after the injection, while those of RIP3- and MLKL- knockout mice appeared completely normal without any observable loss of cells (Figure 6C, 6D).

We also tested the fertility rate of TSZ-treated mice 3-month after the TSZ treatment. Control injection of saline into the testes of wild type mice did not affect the fertility rate and the mice remained 100% fertile, but TSZ injection reduced the fertility rate by 87.5% (only 1 of 8 was fertile) (Figure 6E). In contrast, 6 out of 8 RIP3-knockout mice and 7 out of 8 MLKL-knockout mice were still fertile following TSZ injection (Figure 6E).

An RIP1 kinase inhibitor blocks aging of the male reproductive system

The identification of the role of necroptosis in the aging of the mouse male reproductive system suggests the feasibility of a pharmaceutical intervention against the aging process. We therefore evaluated the effects of a newly-identified, highly-potent, and highly-specific RIP1 kinase inhibitor from our laboratory (henceforth 'RIPA-56')(Ren et al., 2017) by incorporating it into mouse food at 150 mg/kg and 300 mg/kg doses. We first tested the effect of RIPA-56 on necroptosis in testes by injecting TSZ into testes of 2-month old mice after feeding the mice with increasing concentrations of RIPA-56-containing chow for one week. RIPA-56 blocked the appearance of TSZ-induced phospho-MLKL in the testes in a dose-dependent manner, and was able to completely block necroptosis at the 300 mg/kg dose (Figure 7A, lane 4).

We subsequently chose the 300 mg/kg dose to continuously feed 13-month old male wild type mice for two months to study the long-term effects of blocking necroptosis on testes. After two months, the mice feed RIPA-56 weighed less than mice fed with control chow diet (Figure 7B). The seminal vesicles of the RIPA-56-treated mice retained the mass (mostly around 1,000 milligrams), while the seminal vesicles from mice on normal chow grew significantly during the same period, with a majority of them weighing more than 2,000 milligrams (Figure 7C, 7D). Additionally, the testosterone level of RIPA-56-treated mice remained high, while that of control mice decreased (Figure 7E). Consistently, more than 12% of the seminiferous tubules of the control mice were empty, whereas hardly any seminiferous vesicles were empty in the RIPA-56-treated mice (Figure 7F, 7G). Finally, the fertility rates of the RIPA-56-treated mice were much higher than those of control mice with 19 out of 25 mice on the RIPA-56 diet were fertile while only 6 out of 23 mice on normal diet produced progeny (Figure 7H).

Discussion

296 **Necroptosis in testis promotes the aging phenotype of mouse male reproductive system**

297 The above presented data indicated that the previously unknown physiological function of
298 necroptosis is to promote the aging of male reproductive organs. We detected for the first time
299 under physiological conditions the activation marker of necroptosis in spermatogonia of old
300 testis. Consistently, mice with either of their core necroptosis execution components RIP3 and
301 MLKL deleted from their genome showed dramatic delay of male reproductive aging phenotype,
302 both morphologically and functionally.

303 The delay of aging phenotype seems to be restricted to the reproductive system. We
304 conducted histological analysis of major organs including small intestines, spleen, lung, liver,
305 large intestines, kidney, heart, and brain of wild type and RIP3-knockout mice aged 8 weeks, 4
306 months, 18 months, and 24 months, and observed no differences between wild type and age-
307 matched RIP3-knockout mice during the aging process (Figure 1-figure supplement 6).

308 The fact that one dose of TSZ treatment applied locally to the testes could mimic the aging
309 phenotype, including the enlargement of seminal vesicles, the depletion of cells in the
310 seminiferous tubules, and decreases in fertility rates in wild type but not RIP3-knockout or
311 MLKL-knockout mice, strongly suggests that necroptosis happening within seminiferous tubules
312 is the cause of symptomatic male reproductive system aging.

313

314 **Necroptosis-promoted male reproductive system aging offers an evolutionary advantage at**
315 **species level**

316 When we examined the progenies sired by the aged RIP3-knockout mice at a time wild type
317 mice had lost their reproductive activity, we found that they were less healthy than the progenies
318 sired by young males, with higher rates of prenatal and postnatal death (Figure 1-figure

supplement 7A and Figure1-table supplement 1). A study into the possible reason for the unhealthy offspring revealed accumulated oxidative damage in the sperm DNA of aged RIP3-knockout mice, measured as the level of 8-hydroxydeoxyguanosine (8-OHdG), a biomarker for the oxidative damage of DNA (Chigurupati et al., 2008; Johnson et al., 2015; Paul et al., 2011), was significantly higher in the sperm of 18-month old RIP3-knockout mice than in 4-month old mice (Figure 1-figure supplement 7B,7C). Also, considering that the levels of the pituitary hormones LH and FSH declined in RIP3-knockout mice as they age just as they do in wild type mice, it is obvious that other age-related changes in DNA in their gametes and other organs occur normally in these mutant mice. Therefore, although mice without the core components of the necroptosis pathway maintain their reproductive activity into advanced ages (well beyond the age when wild type mice have largely lost such capacity), these age-associated, non-necroptotic changes still caused deleterious effects on their progeny.

We therefore propose that necroptosis in seminiferous tubules is a physiological response to yet-to-be-identified, age-related, TNF family of cytokine(s) that transduces necroptosis signal through the canonical RIP1-RIP3-MLKL pathway. The necroptotic death of cells in seminiferous tubules of testis then triggers the other downstream age-related phenotypes such as enlargement of seminal vesicles, decreased testosterone levels and weight gain. Given the large number of TNF family of cytokines and the signal seems to only act on spermatogonia, the identification of such a signal is a challenge yet interesting research topic for the future studies.

Necroptosis-instigated reproductive system aging effectively eliminates old animals from the reproductive pool. Given that aged animals carry significantly more DNA damage than younger animals, their elimination from the mating pool results in healthier pups on the whole,

an outcome that would confer an evolutionary advantage over (a population) of animals that do not thusly employ a necroptosis program in their testes.

Interestingly, when wild type mice were fed with food containing an RIP1 inhibitor prior to the onset of reproductive system aging (13 months), the aging of the male reproductive system could be completely blocked. This finding not only further confirms that necroptosis is the mechanism underlying male reproductive system aging, but also demonstrates an apparently-effective way to delay it.

Materials and Methods

Mice

The $RIP3^{-/-}$ (RIP3-knockout) mice (C57BL/6 strain) were generated as described previously (He et al., 2009; 2011). The $MLKL^{-/-}$ (MLKL-knockout) mice were generated by co-microinjection of in vitro-translated Cas9 mRNA and gRNA into the C57BL/6 zygotes. Founders were screened with T7E1 assays and were validated by DNA sequencing. Founders were intercrossed to generate bi-allelic $MLKL^{-/-}$ mice. The gRNA sequence used to generate the knockout mice was GTAGCAGTTGCAAATTAGCGTGG. C57BL/6 wild type (WT, $RIP3^{+/+}$) mice were obtained from Vital River Laboratory Co. WT, $RIP3^{-/-}$, and $MLKL^{-/-}$ mice were produced and maintained at the SPF animal facility of the National Institute of Biological Sciences, Beijing. Animals for the aging study were produced by mating wild type males with wild type females purchased from Vital River Laboratory Co; $RIP3^{-/-}$ mice were produced by mating $RIP3^{-/-}$ males with $RIP3^{-/-}$ females; $MLKL^{-/-}$ mice were produced by mating $MLKL^{-/-}$ males with $MLKL^{-/-}$ females. Animals (male) for the aging study were housed under the same

363 conditions after birth. Animals used for the hormone and the fertility tests were housed
364 individually in an SPF barrier facility.

365 **Antibodies and reagents**

366 The Antibody against RIP3 (#2283; WB, 1:1000; IHC, 1:100) were obtained from
367 ProSci. Other antibodies used in this study were: anti-GAPDH-HRP (M171-1, MBL, 1:5000),
368 anti-RIP1 (#3493S, Cell Signaling, 1:2000), anti-MLKL (AO14272B, ABGENT, 1:1000), anti-
369 Mouse-phospho-MLKL (ab196436; WB, 1:1000; IHC, 1:100), anti-GATA-1 (sc-265, IHC,
370 1:200), anti-cleaved-caspase-3 (#9661, Cell Signaling; WB, 1:1000; IHC 1:100), anti-caspase-8
371 (proteintech, 66093-1-Ig, 1:100), anti-cleaved-caspase-8 (8592T, Cell Signaling; IHC 1:100),
372 anti-HSD3B1 (ab150384, 1:200) (Abcam), anti-SMAD3 (MA5-15663, Thermo, 1:200), 8-OHdG
373 (N45.1; Genox; 1:200), and anti-UTF1 (#MAB4337, EMD Millipore, 1:200). DPBS (Dulbecco's
374 Phosphate-Buffered Saline) was purchased from Thermo. Lectin from *Datura stramonium*,
375 Sodium L-lactate, Deoxyribonuclease I from bovine pancreas, and MEM Non-essential Amino
376 Acid Solution (100×) were purchased from Sigma. RIPA-56 (RIP1 inhibitor) was generated as
377 described in Ren et al., 2017.

378 **Cell cultures**

379 Primary testis cells were cultured in DMEM:F12 Medium (Hyclone) supplemented with
380 10% FBS (Invitrogen) and penicillin/streptomycin (Invitrogen).

381 **Harvesting of tissues**

382 Mice were euthanized using avertin (20 mg ml^{-1}). Animals were euthanized one by one
383 immediately before dissection, and the dissection was performed as rapidly as possible by a team
384 of several trained staff members working in concert on a single mouse. Major organs were

385 removed, cut into appropriately-sized pieces, and either flash-frozen in liquid nitrogen and stored
386 at -80°C or placed in formalin (Using Bouin's fixative for testis) for preservation. After several
387 days of formalin fixation at room temperature, tissue fragments were transferred to 70% ethanol
388 and stored at 4°C. Blood was collected by cardiac puncture, and was allowed to coagulate for the
389 preparation of serum.

390 **Western blotting**

391 Western blotting was performed as previously described (Wang et al., 2014). Briefly, cell
392 pellet samples were collected and re-suspended in lysis buffer (100 mM Tris-HCl, pH 7.4, 100
393 mM NaCl, 10% glycerol, 1% Triton X-100, 2 mM EDTA, Roche complete protease inhibitor set,
394 and Sigma phosphatase inhibitor set), incubated on ice for 30 min, and centrifuged at 20,000 × g
395 for 30 min. The supernatants were collected for western blotting. Testes tissue samples were
396 ground and re-suspended in lysis buffer, homogenized for 30 seconds with a Paddle Blender
397 (Prima, PB100), incubated on ice for 30 min, and centrifuged at 20,000 × g for 30 min. The
398 supernatants were collected for western blotting.

399 **ELISA**

400 Mice (male) used for the hormone tests were housed individually in an SPF barrier
401 facility. Mice were sacrificed and blood was clotted for two hours at room temperature before
402 centrifugation at approximately 1,000 × g for 20 minutes. Mice blood sera was collected and
403 assayed immediately or was stored as sample aliquots at -20°C. The testosterone/FSH/LH levels
404 were measured with ELISA kits (BIOMATIK, EKU07605, EKU04284, EKU05693); the SHDG
405 level was measured with an ELISA kit (INSTRUCTION MANUAL, SEA396Mu). The ELISA
406 assays were performed according to the manufacturer's instructions.

Histology, immunohistochemisitry, and immunofluorescence

Paraffin-embedded specimens were sectioned to a 5 μm thickness and were then deparaffinized, rehydrated, and stained with haematoxylin and eosin (H&E) using standard protocols. For preparation of immunohistochemistry samples, sections were dewaxed, incubated in boiling citrate buffer solution for 15 min in plastic dishes, and subsequently allowed to cool down to room temperature over 3 hr. Endogenous peroxidase activity was blocked by immersing the slides in hydrogen peroxide buffer (10%, Sinopharm Chemical Reagent) for 15 min at room temperature and were then washed with PBS. Blocking buffer (1% bovine serum albumin in PBS) was added and the slides were incubated for 2 hr at room temperature. Primary antibody against phospho-MLKL, cleaved-caspase-3, and 8-OHdG was incubated overnight at 4°C in PBS. After 3 washes with PBS, slides were incubated with secondary antibody (polymer-horseradish-peroxidase-labeled anti-rabbit, Sigma) in PBS. After a further 3 washes, slides were analyzed using a diaminobutyric acid substrate kit (Thermo). Slides were counter stained with haematoxylin and mounted in neutral balsam medium (Sinopharm Chemical).

Immunohistochemistry analysis for RIP3 was performed by incubating the tissue slides with the indicated antibodies overnight at 4°C in PBS. After 3 washes with PBS, slides were incubated with DyLight-561 conjugated goat anti-rabbit secondary antibodies (Life) in PBS for 8 hr at 4°C. After additional 3 washes, slides were incubated with HSD3B1, GATA-1, or UTF1 antibody overnight at 4°C in PBS. The slides were then washed 3 more times before incubated with DyLight-488 conjugated goat anti-mouse/rat secondary antibodies (Life) for 2 hr at room temperature in PBS. The slides were then washed in PBS, and cell nuclei were then counter-stained with DAPI (Invitrogen) in PBS. The fluorescence images were observed using a Nikon A1-R confocal microscope.

TSZ injection of testis

WT, RIP3$^{-/-}$, and MLKL$^{-/-}$ mice were anaesthetized with injection of 20µl g^{-1} avertin (20 mg ml^{-1}). The abdomen was opened with surgical scissors and the testes were taken out one-by-one. Each testis was then injected with 20 ng ml^{-1} T in the presence of S (100 nM) and Z (20 µM) (15µl, T: S: Z=1:1:1), or saline, with microliter syringes (50 µl). Each testis was then put back into the cavity, and the abdomen was sutured as descbribed in Hooley et al., 2009). Mice were maintained in an SPF animal facility.

Sperm count

Mice were sacrificed and their epididymides were harvested. Each epididymis was punctured with a 25-gauge needle. Sperm were extruded with tweezers from the epididymis and collected in 2 ml of PBS. The solution was strained with a cell strainer (40 µm, BD Falcon), and 5 µl was taken out and diluted in 95 µl PBS. The number of sperm was counted using a cell-counting chamber under a microscope (Schurmann et al., 2002).

Mating and fertility test

Mice (male) used for the fertility tests were housed individually in an SPF barrier facility. To assess vaginal patency, mice were examined daily from weaning until vaginal opening was observed. The fertility rate of males was determined via a standard method (Cooke and Saunders, 2002; Hofmann et al., 2015) by mating a male with a series of pairs of 10-week old wild type females for 3 months; females were replaced every 2 weeks (females were either from our colony or purchased from Vital River Laboratory Co(C57BL/6)). Each litters was assessed from the date of the birth of pups; when pups were born but did not survive, we counted and recorded the number dead pups; for females that did not produce offspring, the number of pups was

recorded as '0'(did not produce a litter with a proven breeder male for a period of 2 months). The number of male mice with reproductive capacity was recorded.

The reproductive longevity of males was determined by continuously housing 2-month old $RIP3^{+/+}$ and $RIP3^{-/-}$ males with a pairs of 10-week old wild type females, the females being replaced every 2 months, until males ceased reproducing (calculated as the age at birth of the litter less 21 days) (Hofmann et al., 2015).

Isolation of cells from testes

Testes from 8-week old mice were collected using a previously-reported protocol (Chang et al., 2011). Briefly, a testis was placed in Enriched DMEM:F12 (Hyclone) media and placed on ice. After removal of the tunica albuginea of a testis, the seminiferous tubules were dissociated and transferred immediately into 10 mL of protocol enzymatic solution 1. Tubules were incubated for 15-20 min at 35°C in a shaking water bath at 80 oscillations (osc)/min and were then layered over 40 mL 5% Percoll/95% 1× Hank's balanced salt solution in a 50 mL conical tube and allowed to settle for 20 min. Leydig cells were isolated from the top 35 mL of the total volume of Percoll. The bottom 5 mL of Percoll was transferred to a fresh 50 mL conical tube containing 10 mL enzymatic solution 2. Tubules were incubated for 20 min at 35°C and 80 osc/min. After incubation, 3 mL charcoal-stripped FBS was immediately added to halt the digestion. All fractions were mixed and immediately centrifuged at 500 × g at 4°C for 10 min. Pellets were re-suspended in PBS and washed 3 times, then cultured in DMEM:F12(10%FBS) medium at 37°C.

RIPA-56 feeding experiment

RIPA-56 in the AIN93G (LAD3001G) at 150 or 300 mg/kg was produced based on the Trophic Animal Feed High-tech Co's protocol. Cohorts of 13-month old wild type male mice

were fed with AIN93G or AIN93G containing RIPA-56 (RIPA-56:300mg/kg) for 2 months in an SPF facility; each male mouse was then mated with four 10-week old wild type female mice successively. The number of male mice with reproductive capacity were recorded.

Statistical analysis

All experiments were repeated at least twice. Data represent biological replicates. Statistical tests were used for every type of analysis. The data meet the assumptions of the statistical tests described for each figure. Results are expressed as the mean ± s.e.m or S.D. Differences between experimental groups were assessed for significance using a two-tailed unpaired Student's *t*-tests implanted in GraphPad prism5 or Excel software. Fertility rates were assessed for significance using chi-square tests (unpaired, two-tailed) implemented in GraphPad prism5 software. The $*P<0.05$, $**P<0.01$, and $***P<0.001$ levels were considered significant. NS, not significant.

Competing interests

The authors declare no competing interests.

Acknowledgements

We thank Drs. Joseph Goldstein and Michael Brown for critically reading the manuscript and thank Dr. John Snyder and Alex Wang for editing the manuscript.

Additional informatiom

Funding

This work was supported by a National Basic Science 973 grants (2013CB530805) from the Chinese Ministry of Science and Technology and by the Beijing Municipal Commission of Science and Technology. The funders had no role in study design, data collection and interpretation, or the decision to submit the work for publication.

Author Contributions

X.W., D.L. and L.M. conception and design; D.L., T.X., and L.M acquisition of data; Y.S, X.L and Z.Z. synthesized and provided RIPA-56; D.L. and X.W. analysis and interpretation of the data; X.W , and D.L drafting the article. All authors discussed the results and commented on the article.

Ethics

All animal experiments were conducted following the Ministry of Health national guidelines for the housing and care of laboratory animals and were performed in accordance with institutional regulations after review and approval by the Institutional Animal Care and Use Committee at National Institute of Biological Sciences, Beijing.

References:

Cai, Z., Jitkaew, S., Zhao, J., Chiang, H.C., Choksi, S., Liu, J., Ward, Y., Wu, L.G., and Liu, Z.G. (2014). Plasma membrane translocation of trimerized MLKL protein is required for TNF-induced necroptosis. Nat Cell Biol *16*, 55-65.

520 Chang, Y.F., Lee-Chang, J.S., Panneerdoss, S., MacLean, J.A., 2nd, and Rao, M.K. (2011).
521 Isolation of Sertoli, Leydig, and spermatogenic cells from the mouse testis. Biotechniques *51*,
522 341-342, 344.
523 Chen, X., Li, W., Ren, J., Huang, D., He, W.T., Song, Y., Yang, C., Li, W., Zheng, X., Chen, P.*, et*
524 *al.* (2014). Translocation of mixed lineage kinase domain-like protein to plasma membrane leads
525 to necrotic cell death. Cell Res *24*, 105-121.
526 Chigurupati, S., Son, T.G., Hyun, D.H., Lathia, J.D., Mughal, M.R., Savell, J., Li, S.C., Nagaraju,
527 G.P., Chan, S.L., Arumugam, T.V.*, et al.* (2008). Lifelong running reduces oxidative stress and
528 degenerative changes in the testes of mice. J Endocrinol *199*, 333-341.
529 Cho, Y.S., Challa, S., Moquin, D., Genga, R., Ray, T.D., Guildford, M., and Chan, F.K. (2009).
530 Phosphorylation-driven assembly of the RIP1-RIP3 complex regulates programmed necrosis and
531 virus-induced inflammation. Cell *137*, 1112-1123.
532 Christofferson, D.E., and Yuan, J. (2010). Necroptosis as an alternative form of programmed cell
533 death. Curr Opin Cell Biol *22*, 263-268.
534 Cooke, H.J., and Saunders, P.T. (2002). Mouse models of male infertility. Nat Rev Genet *3*, 790-
535 801.
536 Degterev, A., Hitomi, J., Germscheid, M., Ch'en, I.L., Korkina, O., Teng, X., Abbott, D., Cuny,
537 G.D., Yuan, C., Wagner, G.*, et al.* (2008). Identification of RIP1 kinase as a specific cellular
538 target of necrostatins. Nat Chem Biol *4*, 313-321.
539 Finch, C.E., and Girgis, F.G. (1974). Enlarged seminal vesicles of senescent C57BL-6J mice. J
540 Gerontol *29*, 134-138.
541 Gonzales, G.F. (2001). Function of seminal vesicles and their role on male fertility. Asian J
542 Androl *3*, 251-258.

He, S., Wang, L., Miao, L., Wang, T., Du, F., Zhao, L., and Wang, X. (2009). Receptor interacting protein kinase-3 determines cellular necrotic response to TNF-alpha. Cell *137*, 1100-1111.

Hentrich, A., Wolter, M., Szardening-Kirchner, C., Luers, G.H., Bergmann, M., Kliesch, S., and Konrad, L. (2011). Reduced numbers of Sertoli, germ, and spermatogonial stem cells in impaired spermatogenesis. Mod Pathol *24*, 1380-1389.

Hofmann, J.W., Zhao, X., De Cecco, M., Peterson, A.L., Pagliaroli, L., Manivannan, J., Hubbard, G.B., Ikeno, Y., Zhang, Y., Feng, B.*, et al.* (2015). Reduced expression of MYC increases longevity and enhances healthspan. Cell *160*, 477-488.

Holler, N., Zaru, R., Micheau, O., Thome, M., Attinger, A., Valitutti, S., Bodmer, J.L., Schneider, P., Seed, B., and Tschopp, J. (2000). Fas triggers an alternative, caspase-8-independent cell death pathway using the kinase RIP as effector molecule. Nat Immunol *1*, 489-495.

Hooley, R.P., Paterson, M., Brown, P., Kerr, K., and Saunders, P.T. (2009). Intra-testicular injection of adenoviral constructs results in Sertoli cell-specific gene expression and disruption of the seminiferous epithelium. Reproduction *137*, 361-370.

Johnson, S.L., Dunleavy, J., Gemmell, N.J., and Nakagawa, S. (2015). Consistent age-dependent declines in human semen quality: a systematic review and meta-analysis. Ageing research reviews *19*, 22-33.

Jung, H., Roser, J.F., and Yoon, M. (2014). UTF1, a putative marker for spermatogonial stem cells in stallions. PLoS One *9*, e108825.

Meng, L., Jin, W., and Wang, X. (2015). RIP3-mediated necrotic cell death accelerates systematic inflammation and mortality. Proc Natl Acad Sci U S A *112*, 11007-11012.

Murphy, J.M., Czabotar, P.E., Hildebrand, J.M., Lucet, I.S., Zhang, J.G., Alvarez-Diaz, S., Lewis, R., Lalaoui, N., Metcalf, D., Webb, A.I.*, et al.* (2013). The pseudokinase MLKL mediates necroptosis via a molecular switch mechanism. Immunity *39*, 443-453.

567 Newton, K., Sun, X., and Dixit, V.M. (2004). Kinase RIP3 is dispensable for normal NF-kappa Bs,
568 signaling by the B-cell and T-cell receptors, tumor necrosis factor receptor 1, and Toll-like
569 receptors 2 and 4. Molecular and cellular biology *24*, 1464-1469.
570 Paul, C., Nagano, M., and Robaire, B. (2011). Aging results in differential regulation of DNA
571 repair pathways in pachytene spermatocytes in the Brown Norway rat. Biol Reprod *85*, 1269-
572 1278.
573 Pettan-Brewer, C., and Treuting, P.M. (2011). Practical pathology of aging mice. Pathobiol Aging
574 Age Relat Dis *1*.
575 Ren, Y., Su, Y., Sun, L., He, S., Meng, L., Liao, D., Liu, X., Ma, Y., Liu, C., Li, S.*, et al.* (2017).
576 Discovery of a Highly Potent, Selective, and Metabolically Stable Inhibitor of Receptor-
577 Interacting Protein 1 (RIP1) for the Treatment of Systemic Inflammatory Response Syndrome.
578 Journal of medicinal chemistry *60*, 972-986.
579 Robinson, N., McComb, S., Mulligan, R., Dudani, R., Krishnan, L., and Sad, S. (2012). Type I
580 interferon induces necroptosis in macrophages during infection with Salmonella enterica serovar
581 Typhimurium. Nature immunology *13*, 954-962.
582 Rodriguez, D.A., Weinlich, R., Brown, S., Guy, C., Fitzgerald, P., Dillon, C.P., Oberst, A., Quarato,
583 G., Low, J., Cripps, J.G.*, et al.* (2016). Characterization of RIPK3-mediated phosphorylation of
584 the activation loop of MLKL during necroptosis. Cell Death Differ *23*, 76-88.
585 Schurmann, A., Koling, S., Jacobs, S., Saftig, P., Krauss, S., Wennemuth, G., Kluge, R., and
586 Joost, H.G. (2002). Reduced sperm count and normal fertility in male mice with targeted
587 disruption of the ADP-ribosylation factor-like 4 (Arl4) gene. Mol Cell Biol *22*, 2761-2768.
588 Sun, L., Wang, H., Wang, Z., He, S., Chen, S., Liao, D., Wang, L., Yan, J., Liu, W., Lei, X.*, et al.*
589 (2012). Mixed lineage kinase domain-like protein mediates necrosis signaling downstream of
590 RIP3 kinase. Cell *148*, 213-227.

591 Tsai, M.Y., Yeh, S.D., Wang, R.S., Yeh, S., Zhang, C., Lin, H.Y., Tzeng, C.R., and Chang, C.
592 (2006). Differential effects of spermatogenesis and fertility in mice lacking androgen receptor in
593 individual testis cells. Proc Natl Acad Sci U S A *103*, 18975-18980.
594 Upton, J.W., Kaiser, W.J., and Mocarski, E.S. (2010). Virus inhibition of RIP3-dependent necrosis.
595 Cell host & microbe *7*, 302-313.
596 van Bragt, M.P., Roepers-Gajadien, H.L., Korver, C.M., Bogerd, J., Okuda, A., Eggen, B.J., de
597 Rooij, D.G., and van Pelt, A.M. (2008). Expression of the pluripotency marker UTF1 is restricted
598 to a subpopulation of early A spermatogonia in rat testis. Reproduction *136*, 33-40.
599 Vandenabeele, P., Galluzzi, L., Vanden Berghe, T., and Kroemer, G. (2010). Molecular
600 mechanisms of necroptosis: an ordered cellular explosion. Nat Rev Mol Cell Biol *11*, 700-714.
601 Vermeulen, A., Kaufman, J.M., and Giagulli, V.A. (1996). Influence of some biological indexes on
602 sex hormone-binding globulin and androgen levels in aging or obese males. The Journal of
603 clinical endocrinology and metabolism *81*, 1821-1826.
604 Wang, H., Sun, L., Su, L., Rizo, J., Liu, L., Wang, L.F., Wang, F.S., and Wang, X. (2014). Mixed
605 lineage kinase domain-like protein MLKL causes necrotic membrane disruption upon
606 phosphorylation by RIP3. Molecular cell *54*, 133-146.
607 Wang, L., Du, F., and Wang, X. (2008). TNF-alpha induces two distinct caspase-8 activation
608 pathways. Cell *133*, 693-703.
609 Wu, J., Huang, Z., Ren, J., Zhang, Z., He, P., Li, Y., Ma, J., Chen, W., Zhang, Y., Zhou, X.*, et al.*
610 (2013). Mlkl knockout mice demonstrate the indispensable role of Mlkl in necroptosis. Cell
611 research *23*, 994-1006.
612 Zhang, D.W., Shao, J., Lin, J., Zhang, N., Lu, B.J., Lin, S.C., Dong, M.Q., and Han, J. (2009).
613 RIP3, an energy metabolism regulator that switches TNF-induced cell death from apoptosis to
614 necrosis. Science *325*, 332-336.

615 Zhou, W., and Yuan, J. (2014). Necroptosis in health and diseases. Seminars in cell &

616 developmental biology *35*, 14-23.

617

618

619

620

621

622 **Figure**

Figure1

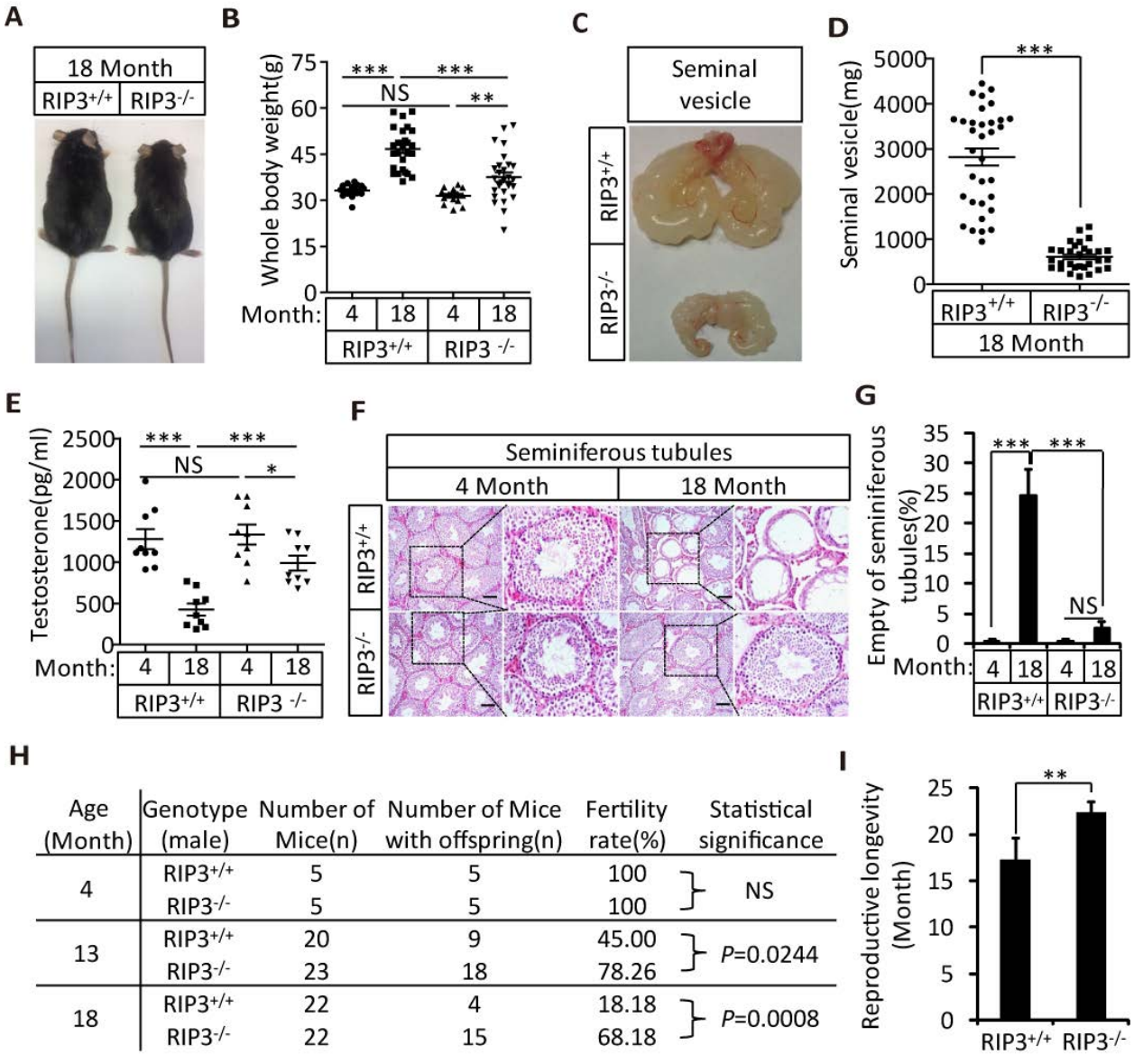

Age (Month)	Genotype (male)	Number of Mice(n)	Number of Mice with offspring(n)	Fertility rate(%)	Statistical significance
4	RIP3$^{+/+}$	5	5	100	NS
	RIP3$^{-/-}$	5	5	100	
13	RIP3$^{+/+}$	20	9	45.00	P=0.0244
	RIP3$^{-/-}$	23	18	78.26	
18	RIP3$^{+/+}$	22	4	18.18	P=0.0008
	RIP3$^{-/-}$	22	15	68.18	

Figure1. RIP3$^{-/-}$ mice maintained their reproductive system function at an advanced age.

(**A**, **B**) Macroscopic features and weights of RIP3$^{+/+}$ (wild type) and RIP3$^{-/-}$ (RIP3 knockout) male mice. RIP3$^{+/+}$ (4 Month, n=16; 18 Month, n=27) and RIP3$^{-/-}$(4 Month, n=16; 18 Month, n=27) male mice were photographed and weighed. Data represent the mean ± the standard error of the mean (s.e.m). $^{**}P<0.01$, $^{***}P<0.001$. P values were determined with unpaired Student's t-tests. NS, not significant.

(**C**, **D**) Macroscopic features and weights of seminal vesicles. Mice were sacrificed at 18 months of age, and the seminal vesicles from $RIP3^{+/+}$ (n=33) and $RIP3^{-/-}$ (n=30) mice were photographed and weighed. Data represent the mean ± s.e.m. ***$P<0.001$. *P* values were determined with unpaired Student's *t*-tests.

(**E**) Serum testosterone levels of mice assayed using ELISA. Mice were sacrificed, and the testosterone levels in serum from $RIP3^{+/+}$ (4 Month, n=9; 18 Month, n=9) and $RIP3^{-/-}$(4 Month, n= 9; 18 Month, n=9) mice were measured using an ELISA kit for testosterone. Data represent the mean ± s.e.m. *$P<0.05$, ***$P<0.001$. *P* values were determined with unpaired Student's *t*-tests. NS, not significant.

(**F**, **G**) H&E of testis sections from $RIP3^{+/+}$ and $RIP3^{-/-}$ mice. $RIP3^{+/+}$ (4 Months, n=10; 18 Months, n=10) and $RIP3^{-/-}$ (4 Months, n=10; 18 Months, n=10) mice were sacrificed and testes were harvested and stained with H&E in (F). The number of empty seminiferous tubules was counted based on H&E staining and quantification in (G), empty seminiferous tubules were counted in 5 fields per testis. Scale bar, 100μm. Data represent the mean ± S.D. ***$P<0.001$. *P* values were determined with unpaired Student's *t*-tests. NS, not significant.

(**H**) Summary of the fertility rates of $RIP3^{+/+}$ and $RIP3^{-/-}$ mice. One male mice of a given age was mated with a pairs of 10-week old wild type female mice for 3 months; females were replaced every 2 weeks. The number of male mice with reproductive capacity was counted (see Materials and Methods). *P* values were determined using chi-square tests.

(**I**) Reproductive longevity. When $RIP3^{+/+}$ (n=12) and $RIP3^{-/-}$ (n=12) male mice were 2 months old, they were continuously mated with a pairs of 10-week old female mice until pregnancies ceased; females were replaced every 2 months. The ages of the males at which their last litter was sired was recorded (calculated as the age at birth of the litter less 21 days, see Materials and

653 Methods). Data represent the mean ± S.D. $**P<0.01$. *P* values were determined with unpaired
654 Student's *t*-tests.

655 The following figure and table supplements are available for figure 1:

656 **Figure 1-figure supplement 1.** Morphological changes in seminal vesicles and testis during
657 aging.

658 **Figure 1-figure supplement 2.**The levels of the pituitary endocrine hormones LH and FSH
659 decline normally in $RIP3^{+/+}$ and $RIP3^{-/-}$ mice.

660 **Figure 1-figure supplement 3.** No morphological differences were apparent in the prostates of
661 $RIP3^{+/+}$ and $RIP3^{-/-}$ mice.

662 **Figure 1-figure supplement 4.** Morphological changes in seminiferous tubules in 36-month old
663 mice.

664 **Figure 1-figure supplement 5.** $RIP3^{-/-}$ mice have higher sperm counts than $RIP3^{+/+}$ mice at an
665 advanced age.

666 **Figure 1-figure supplement 6.** Histological analysis of various organs of $RIP3^{+/+}$ and $RIP3^{-/-}$
667 mice.

668 **Figure 1-figure supplement 7.** Increase of rates of birth defects and oxidative damage in sperm
669 from aged $RIP3^{-/-}$ mice.

670 **Figure 1-table supplement 1.** Summary of the fertility rates and mortality rates of the offspring
671 of 4- or 18-month old $RIP3^{+/+}$ and $RIP3^{-/-}$ male mice.

672 **Figure 1-table supplement 2.** Summary of the fertility rates and mortality rates of the offspring
673 of 13-month old $RIP3^{+/+}$ and $RIP3^{-/-}$ male mice.

674

Figure2

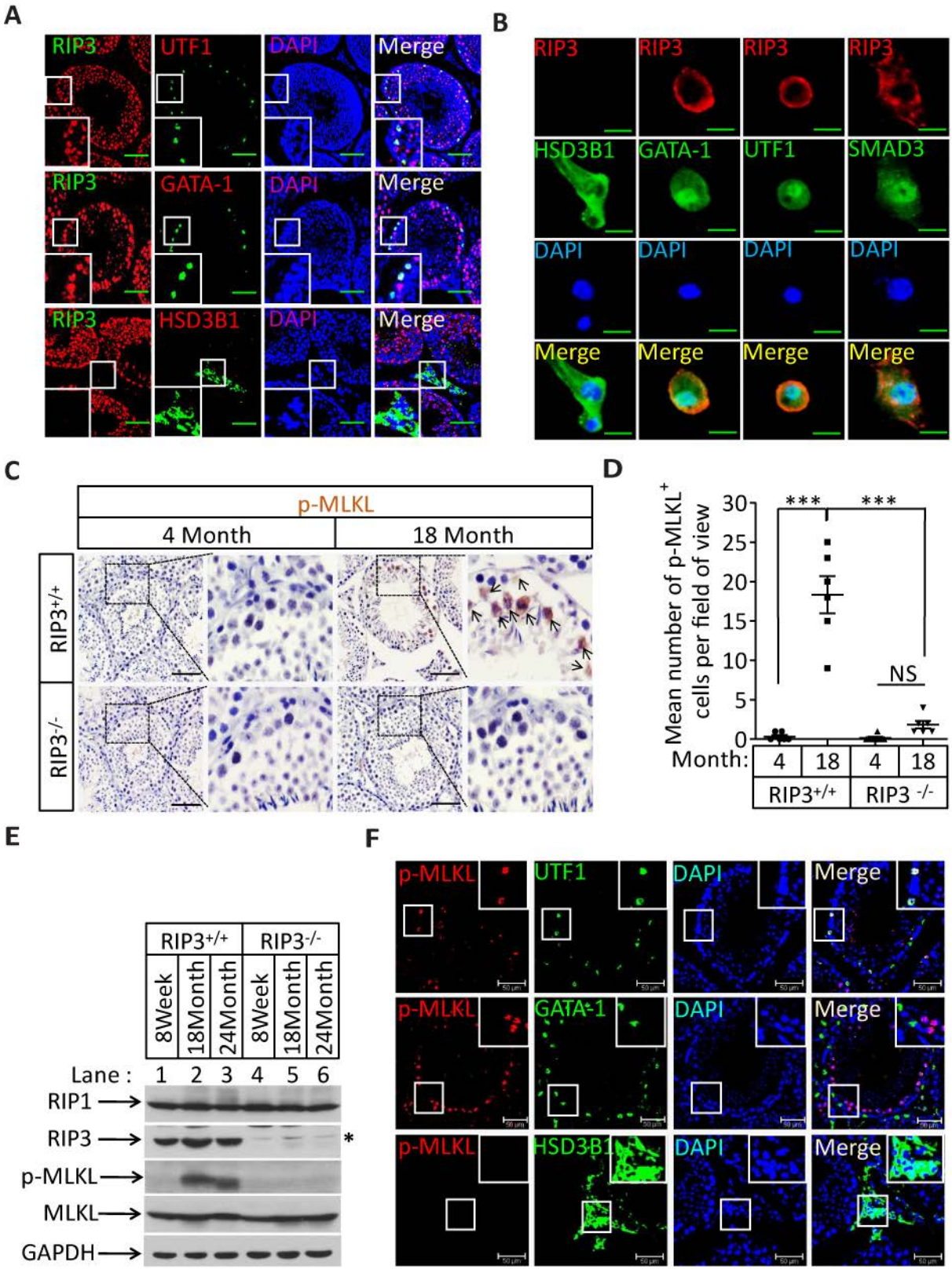

675

Figure 2. Necroptosis in seminiferous tubules of aged wild type mice.

(**A**) RIP3 expression in spermatogonia, Sertoli cells, and spermatocytes. Immunofluorescence in an 8-week old testis with antibodies against RIP3 (red), HSD3B1 (Leydig cells specific protein, green), GATA-1 (Sertoli cells specific protein, green), and UTF1 (spermatogonium specific protein, green). Scale bar, 100μm.

(**B**) RIP3 expression in germ line cells and Sertoli cells. Primary testis cells were isolated from wild type testes, Immunofluorescence of Leydig cells, Sertoli cells, spermatogonia, and primary spermatocytes with antibodies against RIP3 (red), HSD3B1 (green), GATA-1 (green), UTF1 (green), and SMAD3 (primary spermatocytes specific protein, green). Counterstaining with DAPI, blue. Scale bar, 10μm.

(**C**, **D**) Immunohistochemistry (IHC) of testes from $RIP3^{+/+}$ and $RIP3^{-/-}$ mice with phosphor-MLKL (p-MLKL) antibody. $RIP3^{+/+}$ (4 Months, n=6; 18 Months, n=6) and $RIP3^{-/-}$ (4 Months, n=6; 18 Months, n=6) mice were sacrificed and testes were harvested and stained with p-MLKL antibody in (C) (black arrows indicate cells with p-MLKL staining). $p\text{-}MLKL^{+}$ cells were counted in 5 fields per testis and quantification in (D). Scale bar, 100μm. Data represent the mean ± s.e.m. ***$P<0.001$. P values were determined with unpaired Student's t-tests. NS, not significant.

(**E**) Western blot analysis of RIP1, RIP3, MLKL, and p-MLKL levels in the testis after perfusion, each group is representative of at least three mice. GAPDH was used as loading control. The asterisk (*) indicates non-specific bands.

(**F**) Immunofluorescence in an 18-month old testis with antibodies against p-MLKL (red, purple arrows indicate spermatogonium with p-MLKL staining), HSD3B1, GATA-1, and UTF1. Scale bar, 50 μm.

699 The following figure supplements are available for figure 2:

700 **Figure 2-figure supplement 1.** RIP3 expression in seminiferous tubules.

701

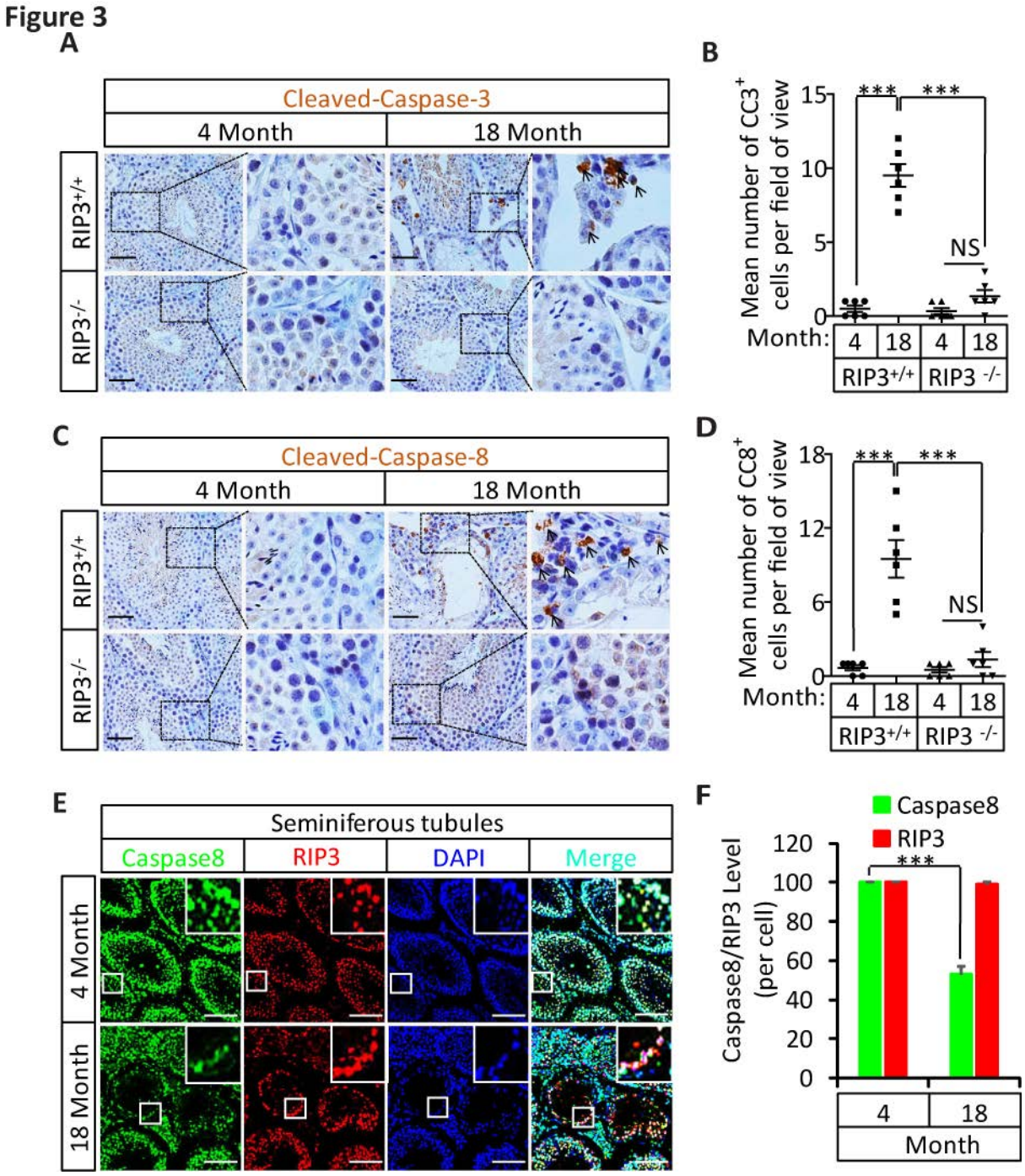

702

Figure 3. Activation of apoptosis in Leydig cells during aging.

(**A**, **B**) IHC of testis from RIP3$^{+/+}$ and RIP3$^{-/-}$ mice with Cleaved-Caspase-3 antibody. Mice were sacrificed, testes from RIP3$^{+/+}$ (4 Month, n=6; 18 Month, n=6) and RIP3$^{-/-}$ (4 Month, n=6; 18 Month, n=6) mice were harvested and stained with Cleaved-Caspase-3 antibody in (A) (black arrows for Leydig cells with Cleaved-Caspase-3 staining). Cleaved-Caspase-3^{+} cells were counted in 6 fields per testis and quantification in (B). Scale bar, 100μm. Data represent the mean ± s.e.m. *$P<0.05$, ***$P<0.001$. *P* values were determined with unpaired Student's *t*-tests.

(**C**, **D**) IHC of testis from RIP3$^{+/+}$ and RIP3$^{-/-}$ mice with Cleaved-Caspase-8 antibody. Mice were sacrificed, testes from RIP3$^{+/+}$ (4 Month, n=6; 18 Month, n=6) and RIP3$^{-/-}$ (4 Month, n=6; 18 Month, n=6) mice were harvested and stained with Cleaved-Caspase-8 antibody in (C) (black arrows for Leydig cells with Cleaved-Caspase-8 staining). Cleaved-Caspase-8^{+} cells were counted in 6 fields per testis and quantification in (D). Scale bar, 100μm. Data represent the mean ± s.e.m. *$P<0.05$, ***$P<0.001$. *P* values were determined with unpaired Student's *t*-tests.

(**E, F**) Caspase8 levels decrease during aging in empty seminiferous tubules. Immunofluorescence of testes from 4-Month old and 18-month old wild type mice with caspase8 and RIP3 antibody in (E). The caspase8 levels were quantified in (F). Counterstaining with DAPI, blue. Scale bar, 100μm.

The following figure supplements are available for figure 3:

Figure 3-figure supplement 1. Activation of apoptosis in Leydig cells during aging.

Figure 3-figure supplement 2. Caspase8 levels increase during aging in Leydig cells.

726

727

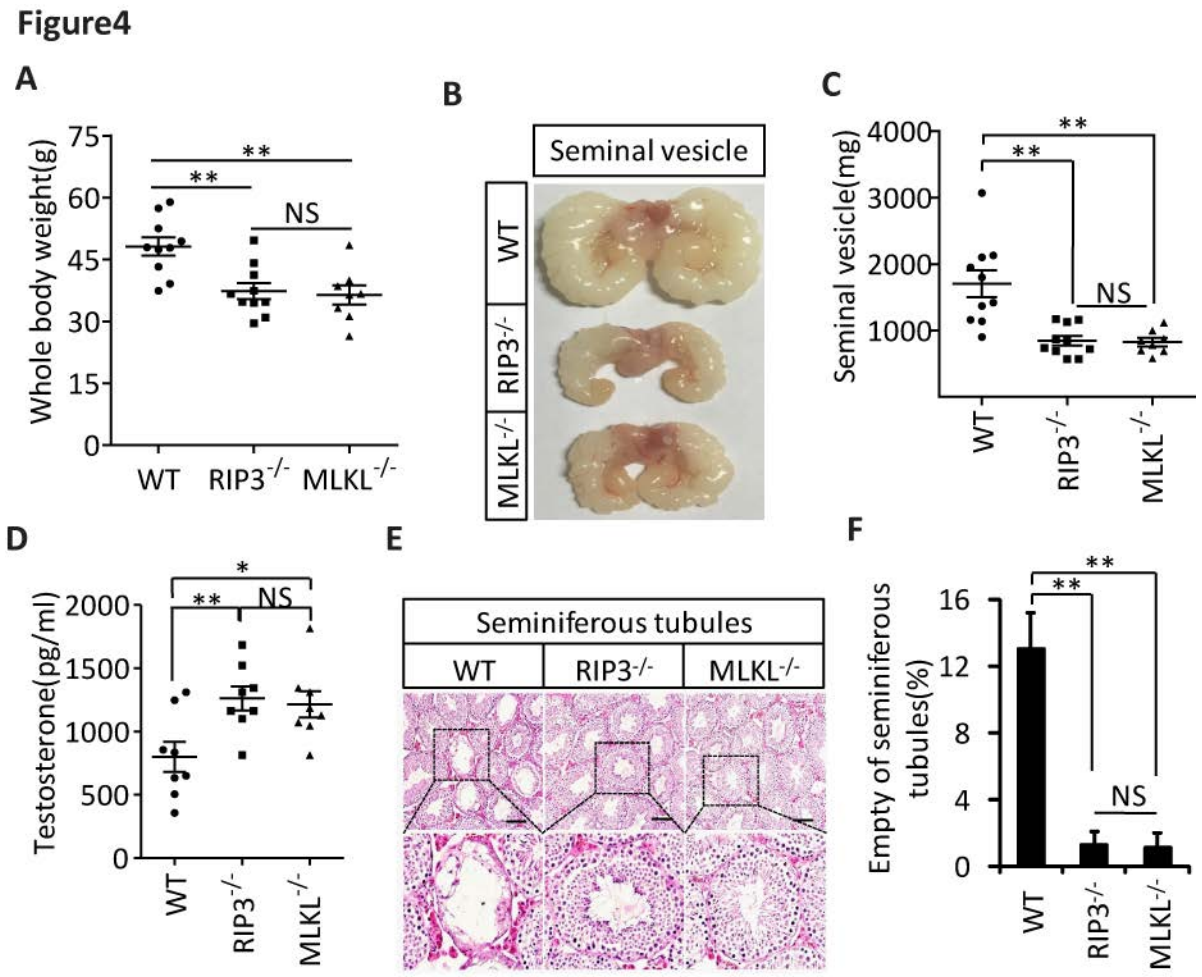

G

Age (Month)	Genotype (male)	Number of Mice(n)	Number of Mice with offspring(n)	Fertility rate(%)	Statistical significance	
16	WT	14	3	21.43	P=0.003	P=0.004
	RIP3-/-	16	13	81.25	NS	
	MLKL-/-	18	14	77.78		

728

729

730 **Figure 4.** Aging of reproductive organs is delayed in MLKL$^{-/-}$ mice.

731 (**A**) Weight of WT (wild type), RIP3$^{-/-}$, and MLKL$^{-/-}$ male mice. WT (15 Month, n=10), RIP3$^{-/-}$

732 (15 Month, n=10) and MLKL$^{-/-}$ (15 Month, n=8) male mice were weighed. Data represent the

mean ± s.e.m. $^{**}P<0.01$. *P* values were determined with unpaired Student's *t*-tests. NS, not significant.

(**B**, **C**) Macroscopic features and weights of seminal vesicles. WT (15 month, n=10), $RIP3^{-/-}$ (15 Month, n=10) and $MLKL^{-/-}$(15 Month, n=8) male mice were sacrificed and the seminal vesicles were photographed and weighed. Data represent the mean ± s.e.m. $^{**}P<0.01$. *P* values were determined with unpaired Student's *t*-tests. NS, not significant.

(**D**) Serum testosterone levels of mice assayed using ELISA. Mice were sacrificed and the level of testosterone in serum from WT (15 Month, n=8), $RIP3^{-/-}$(15 Month, n=8) and $MLKL^{-/-}$(15 Month, n=8) mice was measured using a testosterone ELISA kit. Data represent the mean ± s.e.m. $^{*}P<0.05$, $^{**}P<0.01$. *P* values were determined with unpaired Student's *t*-tests. NS, not significant.

(**E**, **F**) H&E of testis sections from WT, $RIP3^{-/-}$, and $MLKL^{-/}$mice. Testes from WT (15 Months, n=8), $RIP3^{-/-}$ (15 Months, n=8), and $MLKL^{-/-}$(15 Month, n=8) mice were harvested and stained with H&E in (E). The number of empty seminiferous tubules was counted based on H&E staining and quantification in (F), empty seminiferous tubules were counted in 5 fields per testis. Scale bar, 100μm. Data represent the mean ± S.D. $^{**}P<0.01$. *P* values were determined with unpaired Student's *t* tests.

(**G**) Summary of the fertility rates of WT, $RIP3^{+/+}$ and $MLKL^{-/}$mice. One male mice of a given age was mated with a pairs of 10-week old wild type female mice for 3 months; females were replaced every 2 weeks. The number of male mice with reproductive capacity was counted (see Materials and Methods). *P* values were determined using chi-square tests.

Figure5

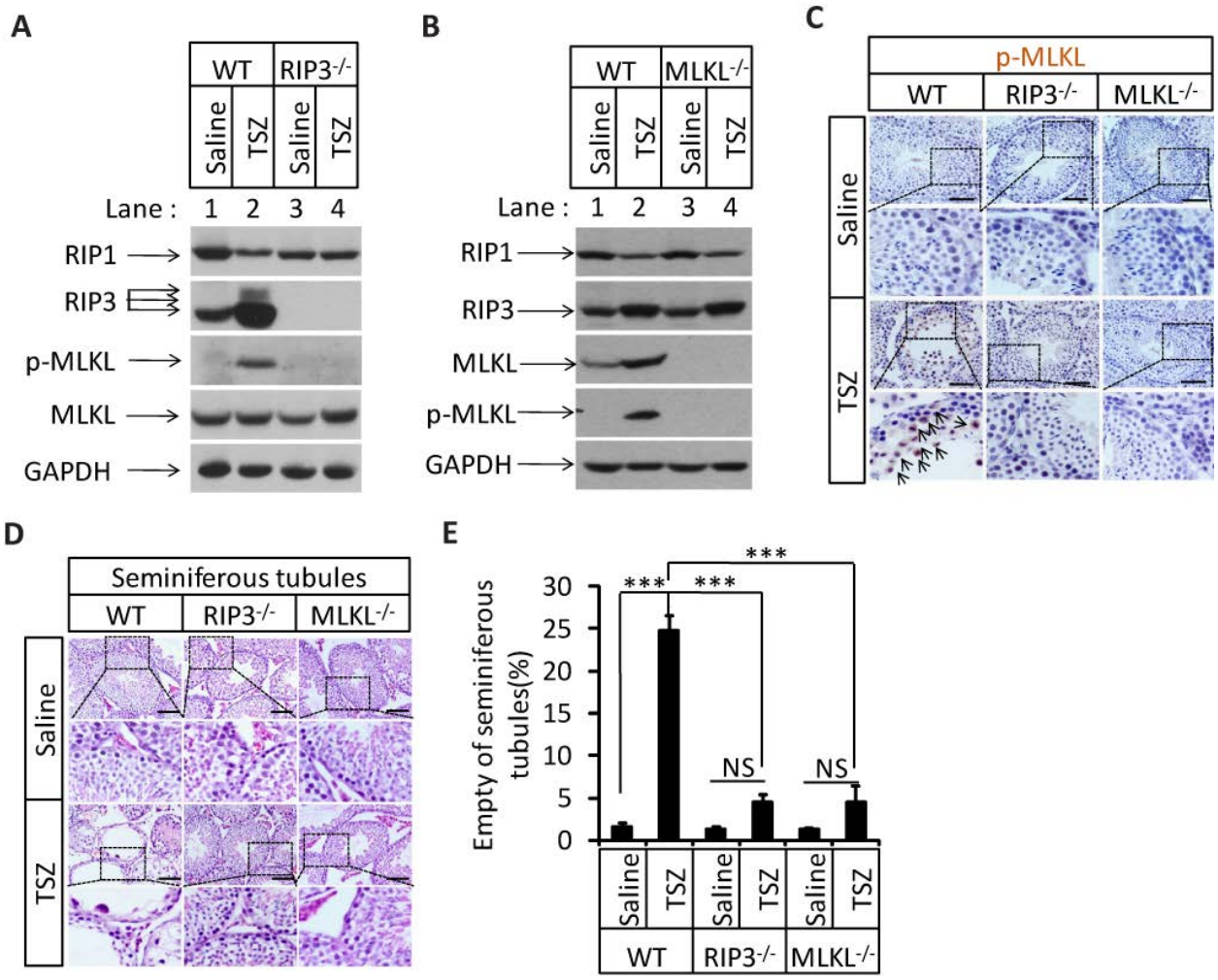

Figure 5. Induction of necroptosis in testis depleted cells in seminiferous tubules.

(**A-E**) Testes of WT (2 Months, n=6), RIP3$^{-/-}$ (2 Months, n=6), and MLKL$^{-/-}$(2 Month, n=6) mice were injected with TSZ or saline (see Materials and Methods); 72 hours after the injection, mice were sacrificed and the testes were harvested. The proteins were extracted from testes and were analyzed with western blotting in (A, B). GAPDH was used as a loading control. The testes were stained with p-MLKL antibody in (C) (black arrows indicate cells with p-MLKL staining). Scale bar, 100μm. The testes were stained with H&E in (D). The number of empty seminiferous

764 tubules was counted based on H&E staining and quantification in (E), empty seminiferous
765 tubules were counted in 5 fields per testis. Scale bar, 100μm. Data represent the mean ±S.D.
766 ***$P<0.001$. *P* values were determined with unpaired Student's *t*-tests. NS, not significant.

767 The following figure supplements are available for figure 5:

768 **Figure 5-figure supplement 1.** Activation of necroptosis in germ line stem cells and Sertoli
769 cells in seminiferous tubules.

770

Figure6

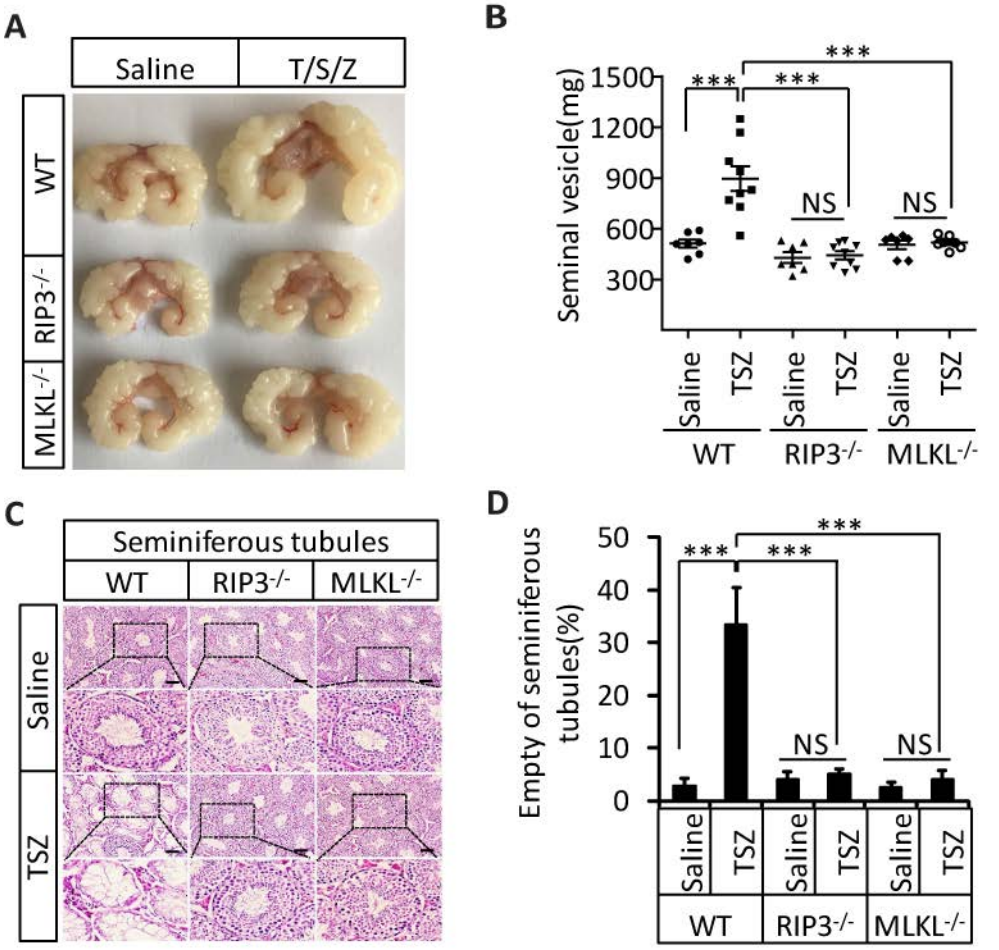

E

Genotype (male)	Injection	Number of Mice(n)	Number of Mice with offspring(n)	Fertility Rate(%)	Statistical significance
WT	Saline	8	8	100	*P*=0.0004
	TSZ	8	1	12.5	
RIP3 -/-	Saline	8	8	100	NS
	TSZ	8	6	75.0	
MLKL -/-	Saline	8	8	100	NS
	TSZ	8	7	87.5	

P=0.0117

P=0.0027

Figure 6. Induction of necroptosis in testes accelerates aging of the male reproductive system.

(**A-D**) Testes from WT (3 Months, n=9), RIP3$^{-/-}$ (3 Months, n= 9), and MLKL$^{-/-}$(3 Month, n=7) mice were injected with TSZ or saline (see Materials and Methods) and were maintained in SPF

facility for 3 months. Mice were then sacrificed and the seminal vesicles were photographed and weighed. Macroscopic features and weights of seminal vesicles form mice in (A, B). Data represent the mean ± s.e.m. ***$P<0.001$, P values were determined with unpaired Student's t-tests. Testes were harvested and stained with H&E in (C). The number of empty seminiferous tubules was counted based on H&E staining and quantification in (D). Empty seminiferous tubules were counted in 5 fields per testis. Scale bar, 100μm. Data represent the mean ± S.D. ***$P<0.001$, P values were determined with unpaired Student's t-tests. NS, not significant.

(**E**) Summary of the fertility rate of WT, RIP3$^{-/-}$, and MLKL$^{-/-}$ male mice after injection with TSZ. Testes from WT (3 Months, n=8), RIP3$^{-/-}$ (3 Months, n=8), and MLKL$^{-/-}$(3 Month, n=8) male mice were injected with TSZ or saline (see Materials and Methods) and mice were maintained in SPF for 3 months. One male mouse was mated with a pairs of 10-week old female wild type mice for 2 months; females were replaced every 2 weeks. The number of male mice with reproductive capacity was counted (see Materials and Methods). P values were determined using chi-square tests.

Figure7

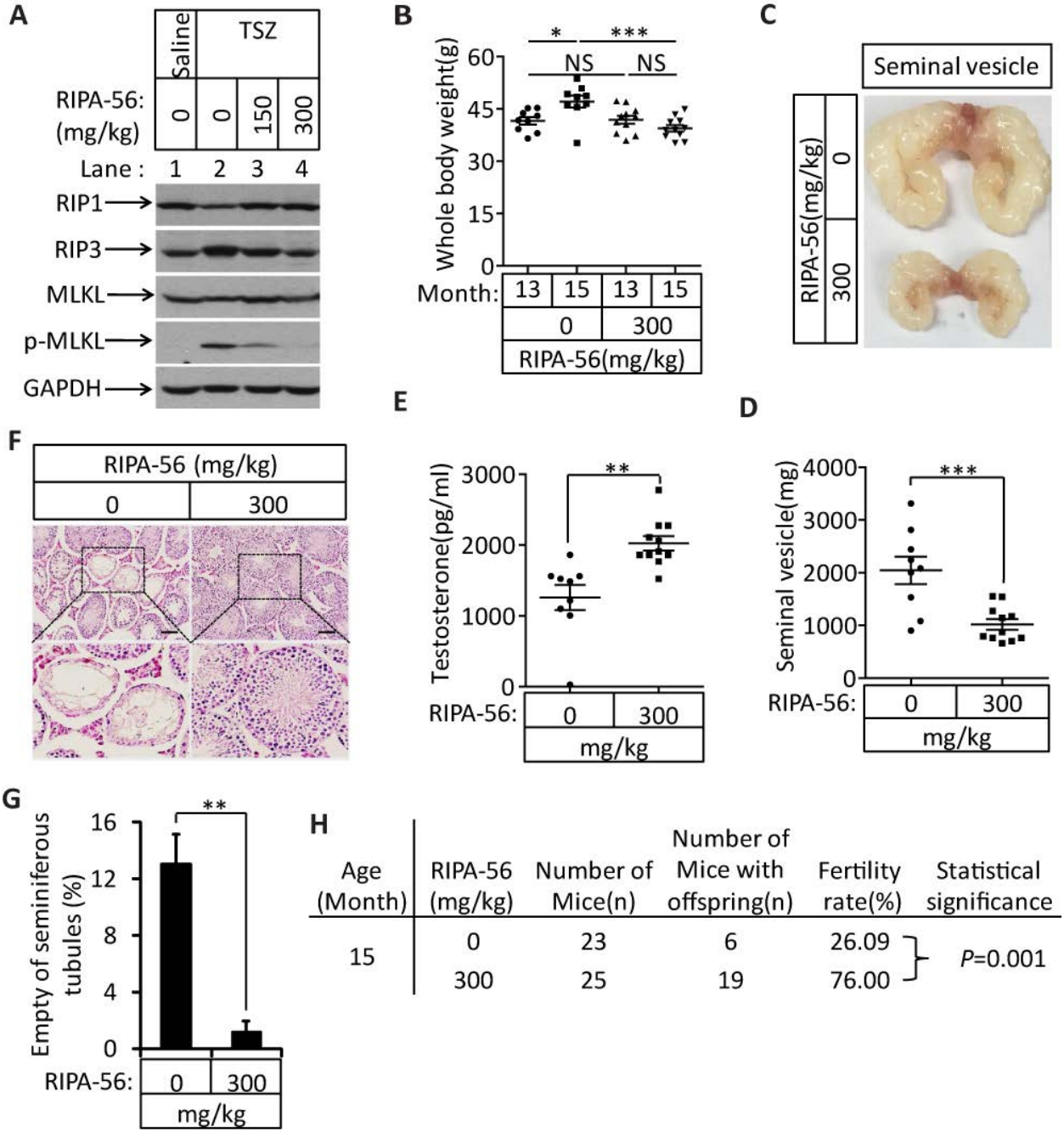

H

Age (Month)	RIPA-56 (mg/kg)	Number of Mice(n)	Number of Mice with offspring(n)	Fertility rate(%)	Statistical significance
15	0	23	6	26.09	*P*=0.001
	300	25	19	76.00	

Figure 7. An RIP1 inhibitor blocks aging of the male reproductive system.

(**A**) Western blot analysis of RIP1, RIP3, MLKL, and p-MLKL levels in testes after injection with TSZ. The 2-month old wild type male mice continuously feed with RIPA-56 (0mg/kg, n=6;

795 150mg/kg, n=3; 300mg/kg, n=3) for one week. Testes were injected with TSZ (see Materials and
796 Methods); 72 hours after the injection, mice were sacrificed and the testes were harvested. The
797 proteins were extracted from testes and were analyzed with western blotting. GAPDH was used
798 as a loading control.
799 (**B-H**) 13-month old wild type male mice were feed with AIN93G (RIPA-56:0mg/kg) or
800 AIN93G-RIPA-56 (RIPA-56:300mg/kg) for 2 months in SPF facility. Mice were weighed before
801 and after feed with RIPA-56 in (B). Data represent the mean ± s.e.m. *$P<0.05$, ***$P<0.001$. P
802 values were determined with unpaired Student's t-tests. Mice were sacrificed and the seminal
803 vesicles were photographed and weighed. Macroscopic features and weights of seminal vesicles
804 form mice in (C, D). Data represent the mean ± s.e.m. ***$P<0.001$. P values were determined
805 with unpaired Student's t-tests. Testosterone levels in serum from mice were measured using a
806 testosterone ELISA kit in (E). Data represent the mean ± s.e.m. **$P<0.01$. P values were
807 determined with unpaired Student's t-tests. The testes were harvested and stained with H&E in
808 (F). The number of empty seminiferous tubules was counted based on H&E staining and
809 quantification in (G). Empty seminiferous tubules were counted in 5 fields per testis. Scale bar,
810 100μm. Data represent the mean ± S.D. **$P<0.01$. P values were determined with unpaired
811 Student's t-tests. The fertility rate of each RIPA-56-treated (0mg/kg, n=23; 300mg/kg,
812 n=25) male mice was assessed by mating it with four 10-week old wild type female mice
813 successively (see Materials and Methods). The number of mice with reproductive capacity was
814 counted in (H). P values were determined using chi-square tests.
815
816
817

818 **Figure Supplement**

Figure1-Figure Supplement 1

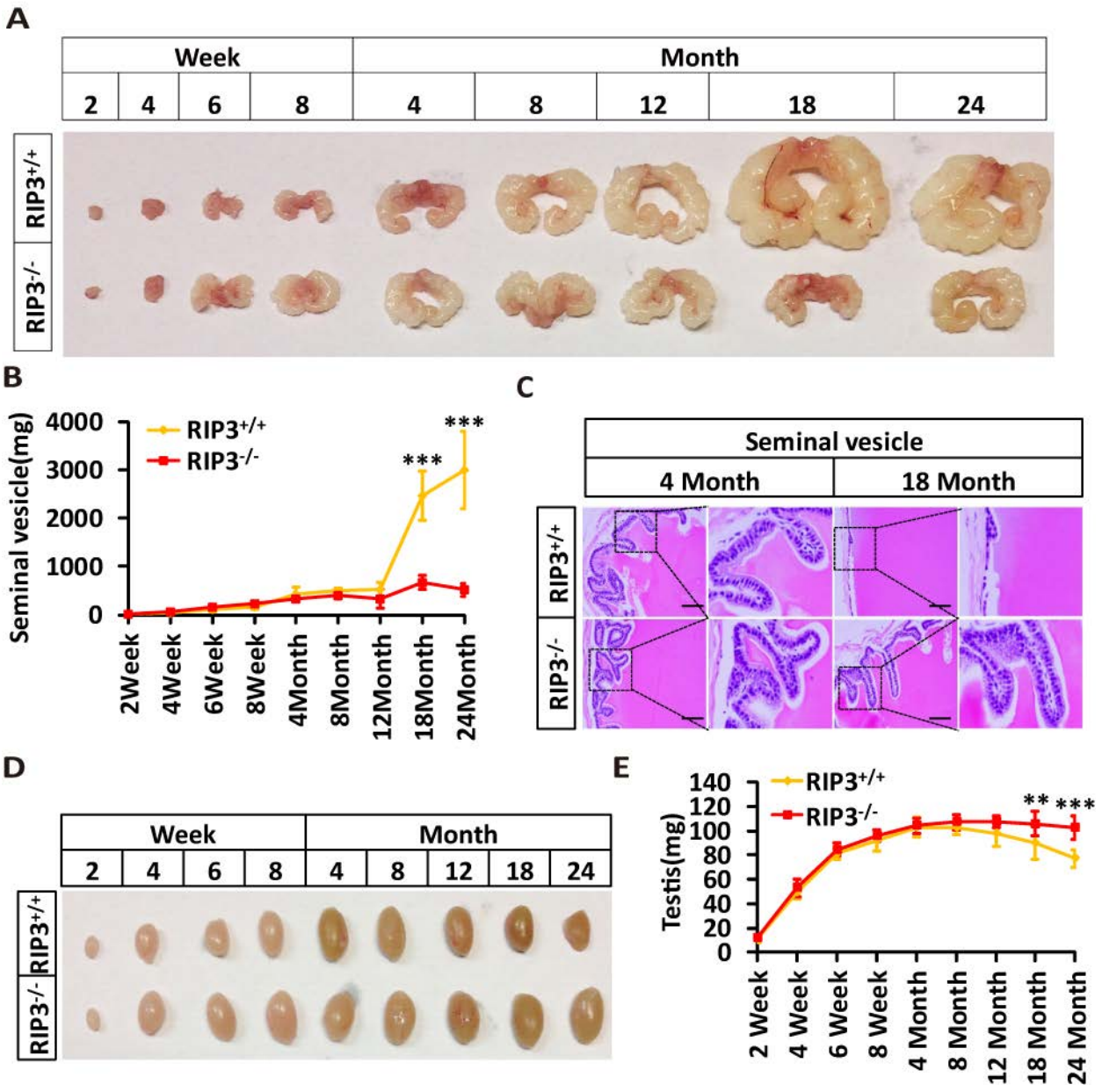

819

820 **Figure 1-figure supplement 1.** Morphological changes in seminal vesicles and testis during

821 aging.

822 (**A**, **B**) Macroscopic features and weights of seminal vesicles at different time points. Mice were

823 sacrificed and the seminal vesicles from $RIP3^{+/+}$ and $RIP3^{-/-}$ mice at different ages were

824 photographed and weighed; each group is representative of at least twelve mice. Data represent
825 the mean ± S.D. ***$P<0.001$. *P* values were determined with unpaired Student's *t*-tests.
826 (**C**) H&E of seminal vesicles sections from $RIP3^{+/+}$ and $RIP3^{-/-}$ male mice. $RIP3^{+/+}$ and $RIP3^{-/-}$
827 mice were sacrificed and seminal vesicles were harvested and stained with H&E; each group is
828 representative of six mice. Scale bar, 50μm.
829 (**D**, **E**) Macroscopic features and weights of testes at different ages. $RIP3^{+/+}$ and $RIP3^{-/-}$ mice of
830 different ages were sacrificed and their testes were photographed and weighed; each group is
831 representative of twelve mice. Data represent the mean ± S.D. **$P<0.01$, ***$P<0.001$. *P*
832 values were determined with unpaired Student's *t*-tests.
833
834
835
836
837

Figure1-Figure Supplement 2

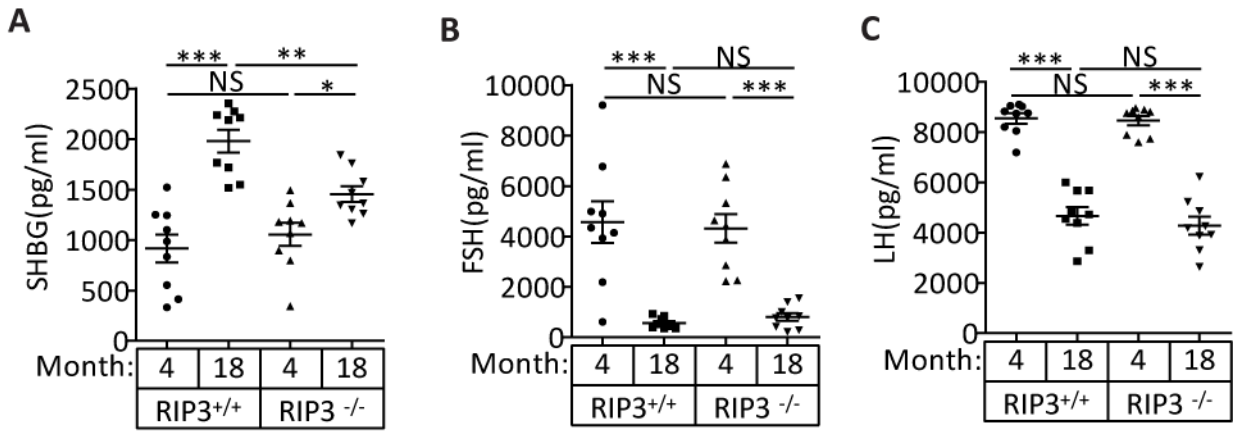

838

839 **Figure 1-figure supplement 2.** The levels of the pituitary endocrine hormones LH and FSH

840 decline normally in RIP3$^{+/+}$ and RIP3$^{-/-}$ mice.

841 (**A**) Serum SHBG levels of mice assayed using ELISA. Mice were sacrificed, and the levels of

842 sex hormone-binding globulin (SHBG) in serum from RIP3$^{+/+}$ (4 Month, n=10; 18 Month, n=10)

843 and RIP3$^{-/-}$(4 Month, n=10; 18 Month, n=10) mice were measured using an SHBG ELISA kit.

844 (**B**) Serum FSH levels of mice assayed using ELISA. Mice were sacrificed, and the follicle-

845 stimulating hormone (FSH) levels in serum from RIP3$^{+/+}$ (4 Month, n=9; 18 Month, n=9) and

846 RIP3$^{-/-}$(4 Month, n=9; 18 Month, n=9) mice were measured using a FSH ELISA kit.

847 (**C**) Serum LH levels of mice assayed using ELISA. Mice were sacrificed, and the luteinizing

848 hormone (LH) levels in serum from RIP3$^{+/+}$ (4 Month, n=9; 18 Month, n=9) and RIP3$^{-/-}$(4

849 Month, n=9; 18 Month, n=9) mice was measured using an LH ELISA kit.

850 All graphs present the mean ± s.e.m. $^{**}P<0.01$, $^{***}P<0.001$. P values were determined with

851 unpaired Student's *t*-tests. NS, not significant.

852

Figure1-Figure Supplement 3

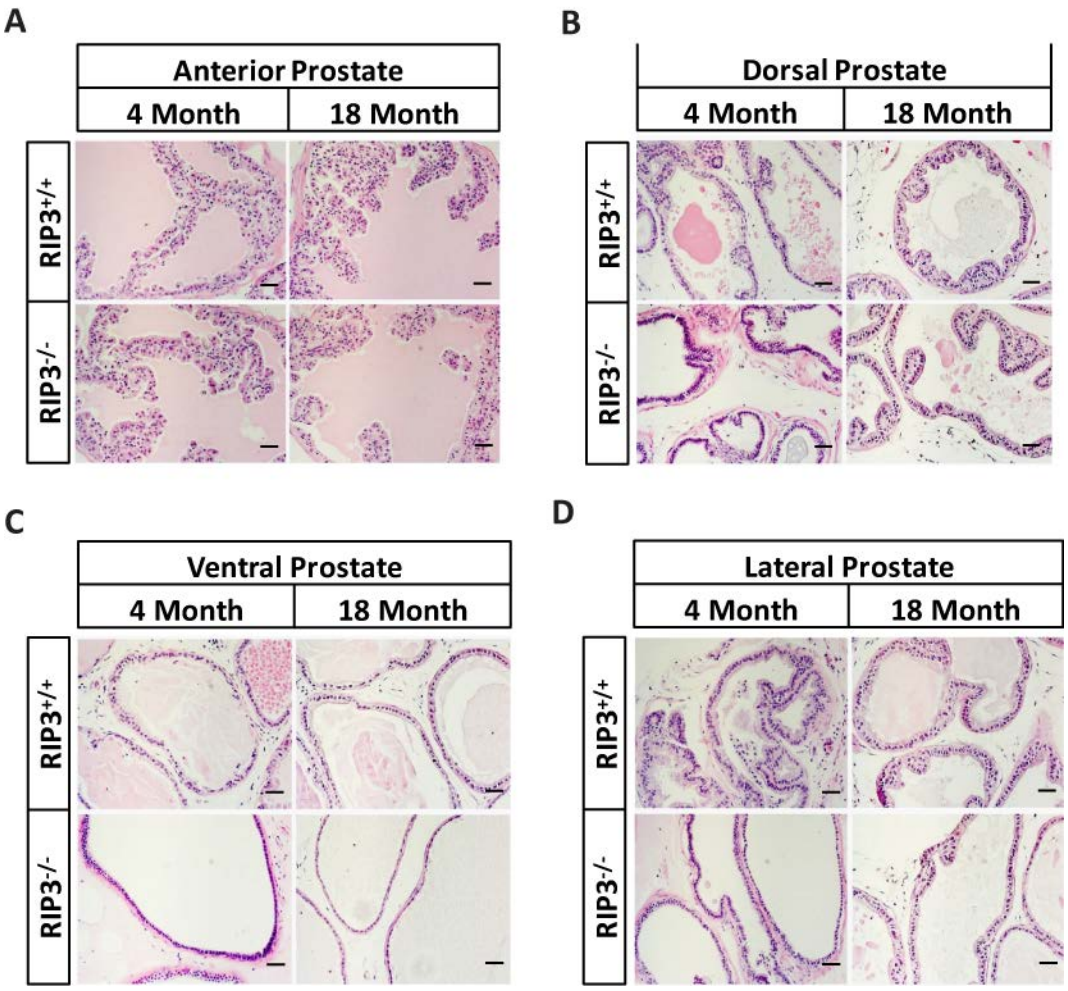

853

854

855 **Figure 1-figure supplement 3.** No morphological differences were apparent in the prostates of

856 $RIP3^{+/+}$ and $RIP3^{-/-}$ mice.

857 (**A-D**) H&E of Anterior/Dorsal/Ventral/Lateral prostate sections from $RIP3^{+/+}$ and $RIP3^{-/-}$ mice.

858 Mice were sacrificed, prostates from $RIP3^{+/+}$ and $RIP3^{-/-}$ mice were harvested and stained with

859 H&E; each group is representative of six mice. Scale bar, 50μm.

860

Figure1-Figure Supplement 4

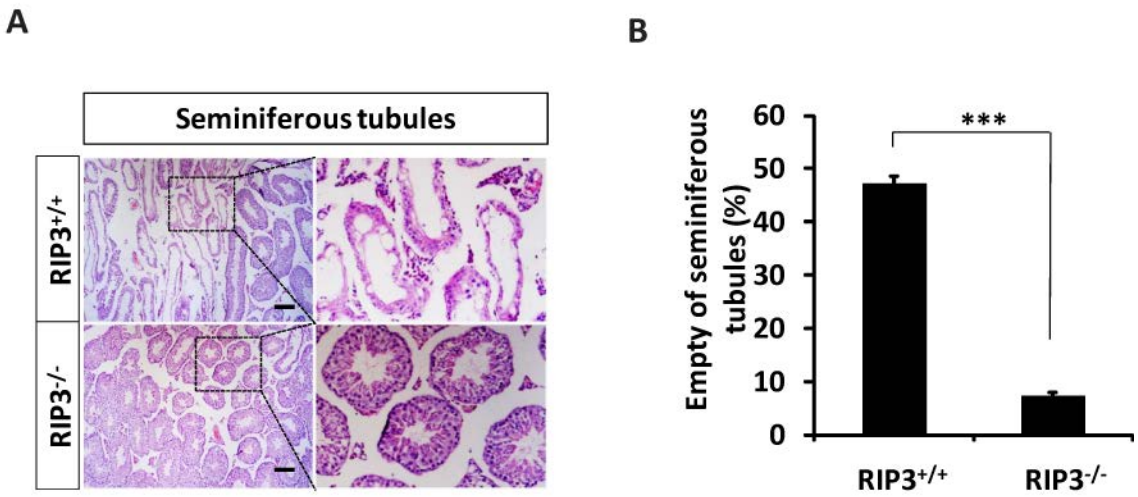

Figure 1-figure supplement 4. Morphological changes in seminiferous tubules in 36-month old mice.

(**A**, **B**) H&E of testis sections from RIP3$^{+/+}$ and RIP3$^{-/-}$ mice. Mice were sacrificed, testes from RIP3$^{+/+}$ (36 Months, n=6) and RIP3$^{-/-}$ (36 Months, n=6) mice were harvested and stained with H&E in (A). The number of empty seminiferous tubules was counted based on H&E staining and quantification in (B), empty seminiferous tubules were counted in 5 fields per testis. Scale bar, 200μm. Data represent the mean ± s.e.m. ***$P<0.001$. *P* values were determined with unpaired Student's *t*-tests.

Figure1-Figure Supplement 5

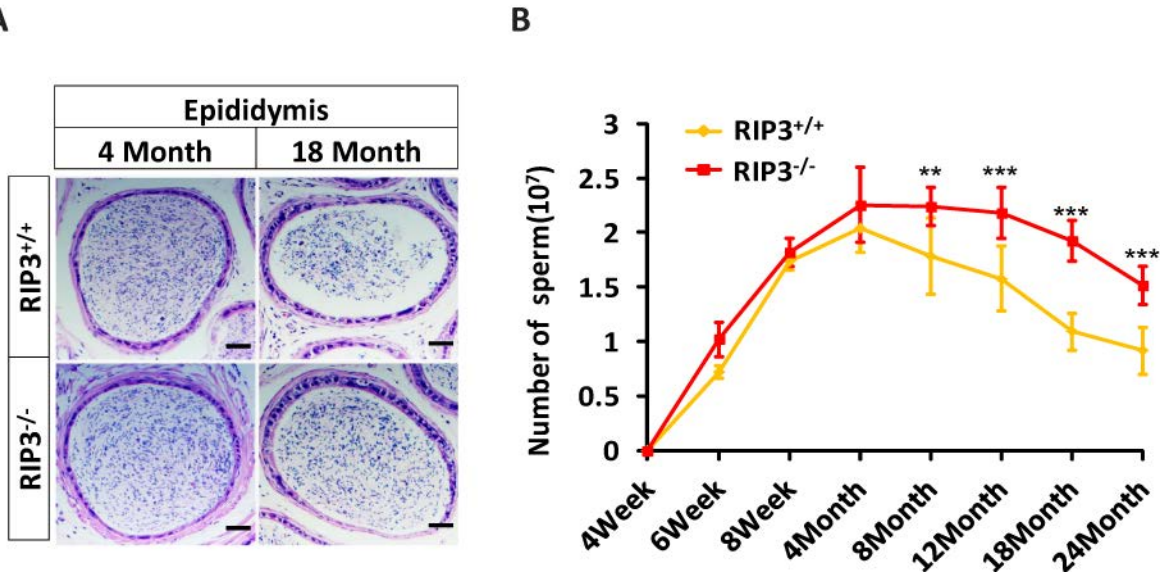

Figure 1-figure supplement 5. RIP3$^{-/-}$ mice have higher sperm counts than RIP3$^{+/+}$ mice at an advanced age.

(**A**) H&E of epididymis sections from RIP3$^{+/+}$ and RIP3$^{-/-}$ mice. Mice were sacrificed and epididymides from RIP3$^{+/+}$ (4 Month, n=6; 18 Months, n=6) and RIP3$^{-/-}$ (4 Month, n=6; 18 Months, n=6) mice were harvested and stained with H&E. Scale bar, 50μm.

(**B**) Sperm count. Mice were sacrificed, and epididymides from RIP3$^{+/+}$ and RIP3$^{-/-}$ mice of at different ages were harvested. The number of sperm within the epididymis was counted using a cell counting chamber under a microscope; each group is representative of at least twelve mice. Data represent the mean ± S.D. $^{**}P<0.01$, $^{***}P<0.001$. *P* values were determined with unpaired Student's *t*-tests.

Figure1-Figure Supplement 6

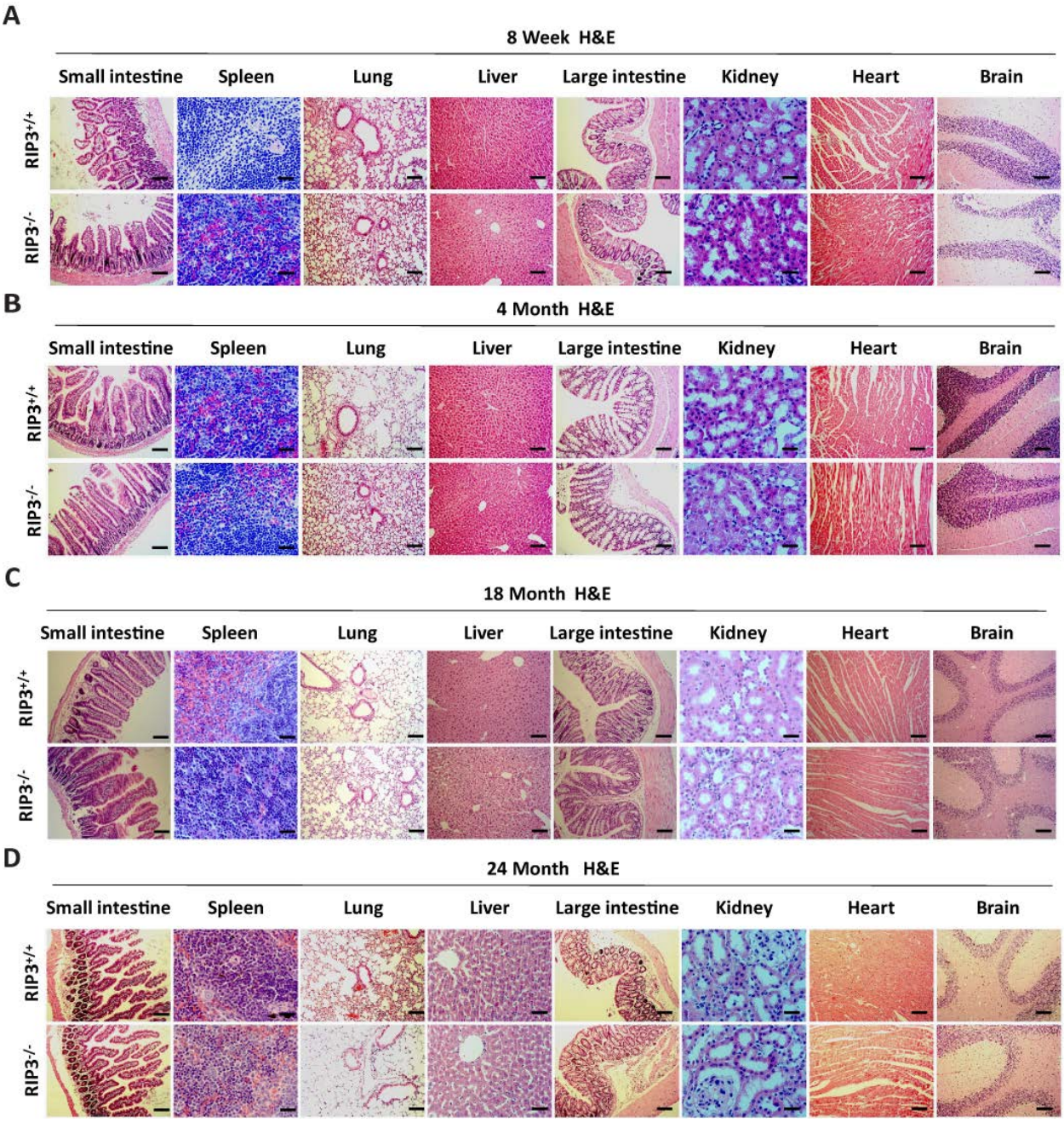

Figure 1-figure supplement 6. Histological analysis of various organs of $RIP3^{+/+}$ and $RIP3^{-/-}$ mice.

887 (**A-D**) H&E of tissue sections from RIP3$^{+/+}$ and RIP3$^{-/-}$ male mice. Mice of different ages were
888 sacrificed, the organs from RIP3$^{+/+}$ and RIP3$^{-/-}$ mice were harvested and stained with H&E; each
889 group is representative of at least six mice. Scale bar, 100μm.

Figure1-Figure Supplement 7

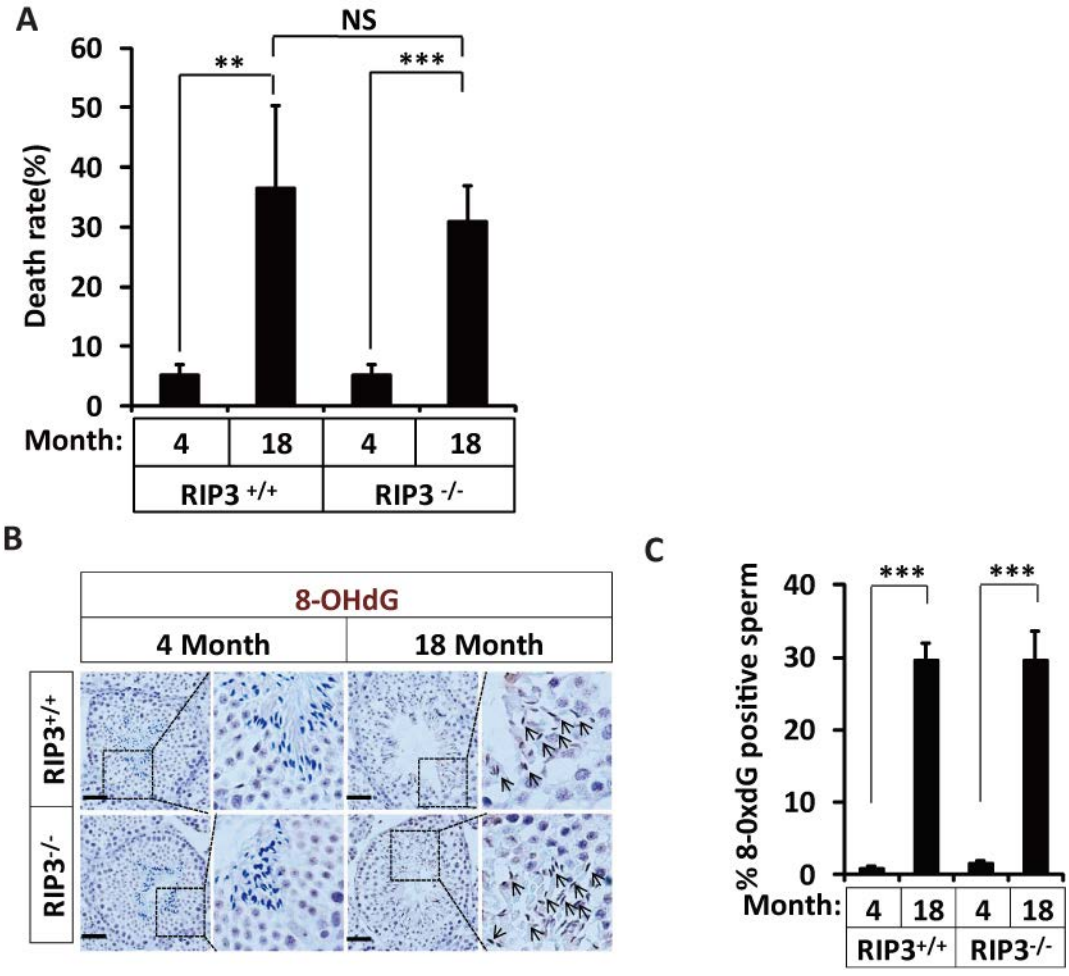

890

891 **Figure 1-figure supplement 7.** Increase of rates of birth defects and oxidative damage in sperm
892 from aged RIP3$^{-/-}$ mice.

893 (**A**) Mortality of offspring from RIP3$^{+/+}$ and RIP3$^{-/-}$ male mice. One male mice of a given age
894 was mated with a pairs of 10-week old female wild type mice for 3 months; females were
895 replaced every 2 weeks. Litters were counted by date of birth of the pups; if a litter was born but

did not survive, we counted the dead pups; if we were not able to count the pups, the number of pups was entered as '0'. Mortality of offspring from 4-month old $RIP3^{+/+}$ (n=5) and $RIP3^{-/-}$ (n=5) male mice; offspring from 18-month old $RIP3^{+/+}$ (n=4) and $RIP3^{-/-}$ (n=15) male mice were calculated. Data represent the mean ± S.D. $^{**}P<0.01$, $^{***}P<0.001$. *P* values were determined with unpaired Student's *t*-tests. NS, not significant.

(**B**, **C**) IHC of $RIP3^{+/+}$ and $RIP3^{-/-}$ testes with 8-OHdG antibody. Mice were sacrificed, testes from $RIP3^{+/+}$ (4 Months, n=6; 18 Months, n=6) and $RIP3^{-/-}$(4 Months, n=6; 18 Months, n=6) mice were harvested and stained with 8-OHdG antibody in (B) (black arrows for sperm with 8-OHdG staining). 8-OHdG^{+} sperm were counted in 5 fields per testis and quantification in (C). Scale bar, 100μm. Data represent the mean ±S.D. $^{***}P<0.001$. *P* values were determined with unpaired Student's *t*-tests.

Figure2-Figure Supplement 1

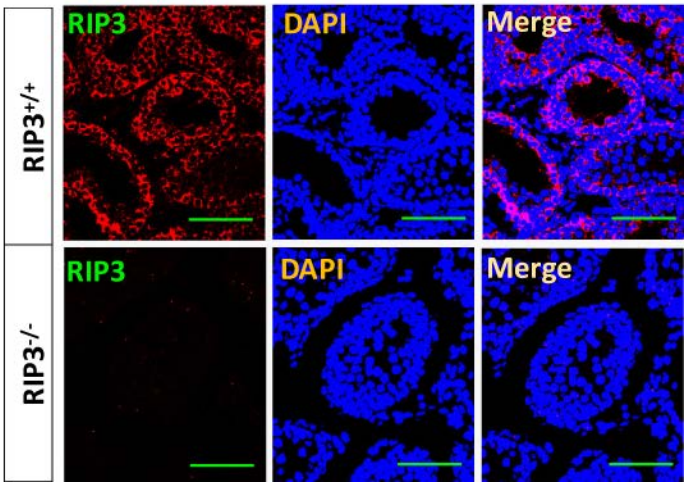

Figure 2-figure supplement 1. RIP3 expression in seminiferous tubules.

Immunofluorescence of testes from $RIP3^{+/+}$ and $RIP3^{-/-}$ mice (2 weeks) with RIP3 antibody. Counterstaining with DAPI, blue. Scale bar, 100μm.

Figure3-Figure Supplement 1

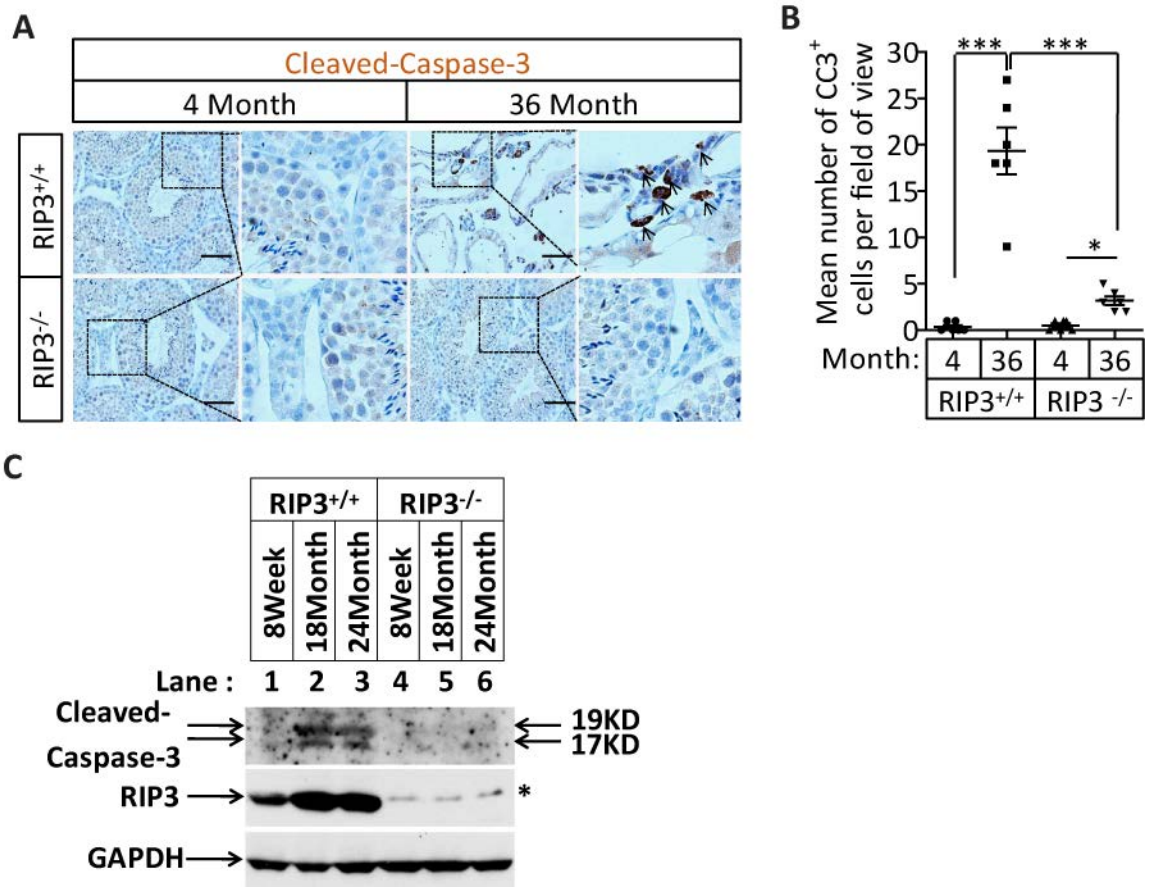

Figure 3-figure supplement 1. Activation of apoptosis in Leydig cells during aging.

(**A**, **B**) IHC of testis from RIP3$^{+/+}$ and RIP3$^{-/-}$ mice with Cleaved-Caspase-3 antibody. Mice were sacrificed, testes from RIP3$^{+/+}$ (4 Month, n=6; 36 Months, n=6) and RIP3$^{-/-}$ (4 Month, n=6; 36 Months, n=6) mice were harvested and stained with Cleaved-Caspase-3 antibody in (A) (black arrows for Leydig cells with Cleaved-Caspase-3 staining). Cleaved-Caspase-3^{+} cells were counted in 6 fields per testis and quantification in (B). Scale bar, 100μm. Data represent the mean ± s.e.m. *$P<0.05$, ***$P<0.001$. P values were determined with unpaired Student's t-tests.

934 (**C**) Western blot analysis of RIP3 and Cleaved-Caspase-3 levels in the testis after perfusion;
935 each group is representative of at least three mice. GAPDH was used as a loading control.
936

Figure3-Figure Supplement 2

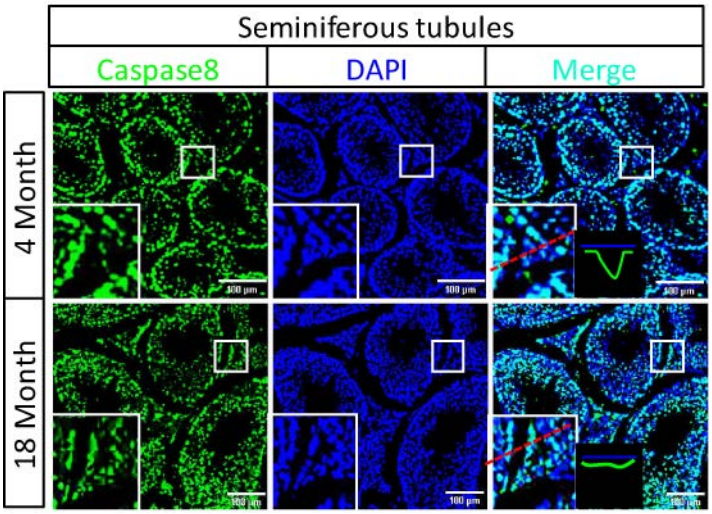

937
938

939 **Figure 3-figure supplement 2.** Caspase8 levels increase during aging in Leydig cells.
940 Immunofluorescence of testes from 4-Month old and 18-month old wild type mice with caspase8
941 antibody. Counterstaining with DAPI, blue. Scale bar, 100μm.

Figure5-Figure Supplement 1

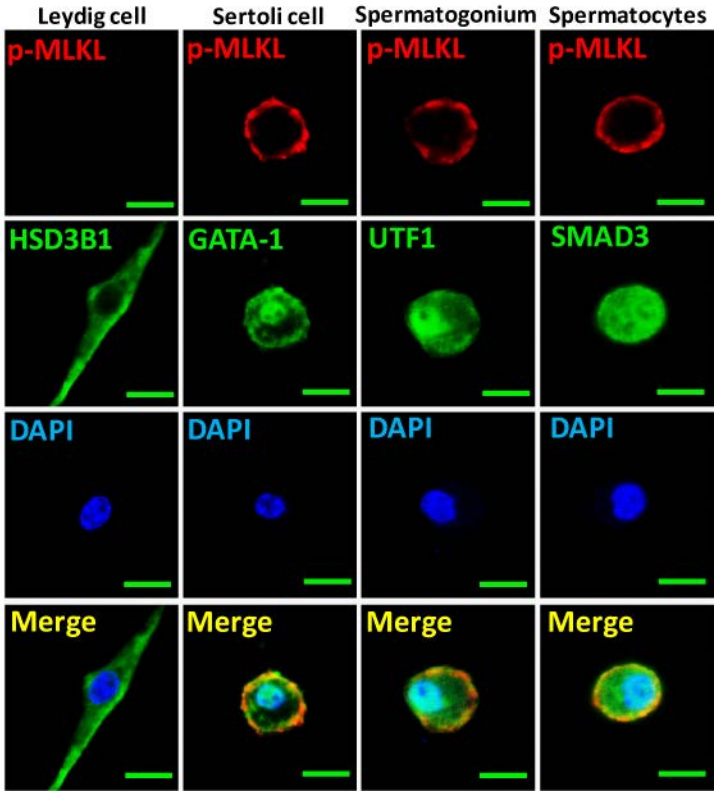

Figure 5-figure supplement 1. Activation of necroptosis in germ line stem cells and Sertoli cells in seminiferous tubules.

Primary testis cells were isolated from wild type testes, immunofluorescence of Leydig cells, Sertoli cells, spermatogonia, and primary spermatocytes with antibodies against p-MLKL (red), HSD3B1 (green), GATA-1 (green), UTF1 (green), and SMAD3 (green) after stimulation with TSZ for 10 hours. Counterstaining with DAPI, blue. Scale bar, 10μm.

Figure1-Table supplement 1. Summary of the total fertility rates and mortality rates of the offspring of 4- or 18-month old $RIP3^{+/+}$ and $RIP3^{-/-}$ male mice.

$RIP3^{+/+}$ (male,4 Month)					$RIP3^{-/-}$ (male,4Month)				
Mice no.	pregnancies times(n) (females)	pups	pups death(n)	Death rate	Mice no.	pregnancies times(n) (females)	pups	pups death(n)	Death rate
#1	4	26	1	3.85	#1	4	30	2	6.67
#2	6	40	2	5.00	#2	4	27	1	3.70
#3	4	28	1	3.57	#3	6	47	3	6.38
#4	4	27	2	7.41	#4	6	37	2	5.41
#5	5	31	2	6.45	#5	5	34	2	5.88
Male fertility rate:100%;Death rate:(5.26±1.65） %					Male fertility rate:100%;Death rate:(5.26±1.66)%				
$RIP3^{+/+}$ (male,18 Month)					$RIP3^{-/-}$ (male,18Month)				
Mice no.	pregnancies times(n) (females)	pups	pups death(n)	Death rate	Mice no.	pregnancies times(n) (females)	pups	pups death(n)	Death rate
#1	2	14	8	57.14	#1	2	18	7	38.89
#2	0	0	0	0	#2	4	34	10	29.41
#3	0	0	0	0	#3	0	0	0	0
#4	2	17	5	29.41	#4	7	61	19	31.15
#5	0	0	0	0	#5	3	25	8	32.00
#6	0	0	0	0	#6	4	33	10	30.30
#7	0	0	0	0	#7	0	0	0	0
#8	3	24	7	29.17	#8	0	0	0	0
#9	0	0	0	0	#9	0	0	0	0
#10	0	0	0	0	#10	3	24	7	29.17
#11	0	0	0	0	#11	0	0	0	0
#12	0	0	0	0	#12	2	19	5	26.32
#13	0	0	0	0	#13	0	0	0	0
#14	0	0	0	0	#14	2	16	4	25.00
#15	0	0	0	0	#15	0	0	0	0
#16	0	0	0	0	#16	2	15	6	40.00
#17	3	20	6	30.00	#17	3	28	5	17.86
#18	0	0	0	0	#18	2	12	3	25.00
#19	0	0	0	0	#19	3	30	12	40.00
#20	0	0	0	0	#20	2	19	6	31.58
#21	0	0	0	0	#21	3	23	7	30.43
#22	0	0	0	0	#22	3	26	9	34.62
Male fertility rate:18.18%;Death rate:(36.43±13.81)%					Male fertility rate:68.18%;Death rate:(30.78±6.04)%				

Figure 1-table supplement 1. Summary of the fertility rates and mortality rates of the offspring of 4- or 18-month old $RIP3^{+/+}$ and $RIP3^{-/-}$ male mice.

Figure1-Table supplement 2. Summary of the total fertility rates and mortality rates of the offspring of 13-month old $RIP3^{+/+}$ and $RIP3^{-/-}$ male mice.

$RIP3^{+/+}$ (male,13 Month)			$RIP3^{-/-}$ (male,13Month)		
Mice no.	pregnancies times(n) (females)	pups	Mice no.	pregnancies times(n) (females)	pups
#1	0	0	#1	5	34
#2	5	53	#2	8	56
#3	6	44	#3	5	48
#4	8	55	#4	7	56
#5	0	0	#5	9	66
#6	6	24	#6	0	0
#7	7	49	#7	14	90
#8	5	31	#8	8	58
#9	6	37	#9	6	31
#10	0	0	#10	10	66
#11	5	33	#11	8	54
#12	0	0	#12	4	14
#13	0	0	#13	2	18
#14	0	0	#14	9	70
#15	0	0	#15	7	40
#16	0	0	#16	0	0
#17	0	0	#17	0	0
#18	0	0	#18	0	0
#19	0	0	#19	0	0
#20	5	29	#20	4	27
			#21	9	57
			#22	8	59
			#23	7	50
Male fertility rate:45.00%			Male fertility rate:78.26%		

Figure 1-table supplement 2. Summary of the fertility rates and mortality rates of the offspring of 13-month old $RIP3^{+/+}$ and $RIP3^{-/-}$ male mice.